DRIVE TUBES 74002/74001

Dissection and description by J. Stewart Nagle
27 January, 1978

* * * * * * * * * * *

LIST OF TABLES

* * * * * * * * * * *

LIST OF ILLUSTRATIONS

APPENDIX

DRIVE TUBES 74002-74001

INTRODUCTION

Drive tubes 74002 and 74001 represent the upper and lower halves of a double drive tube, taken at the rim of Shorty Crater. These cores recovered a total of 68.1 cm of soil column, providing depth coverage that the nearby trench, only 5-8 cm deep, could not.

These drive tubes are unusual in containing relatively homogeneous, orange and black soil of distinctive petrography and composition, and not mixed with components from the surrounding regolith. Because of their unusual nature, the colored glass soils at Shorty Crater have been some of the most-studied material returned from the moon (Meyer et al. 1975). The orange and light-colored soils were collected from a shallow excavation that trenched across the orange glass deposit, and the black (very dark in aggregate) devitrified glasses were found in the lower part of the double drive tube. A thin, half-cm layer of grey mantling surficial soil was expected at the top of the core (Bailey & Ulrich 1975, p. 153).

Because of the unusual cohesiveness and high density of the colored glass deposit, more than 28 hammer blows were needed to pound the tube to its maximum depth. The cohesiveness of the soil, however, made sample recovery unusually good, and the drive tubes were filled beyond design capacity. Although the cohesiveness hindered extraction of the core from the drive tubes, the unusually fine grain size and compositional uniformity expedited rapid processing of the opened core. A review of the geologic setting of the sample site and then the results of this sampling and processing activity are given below.

RELATIONSHIP TO SAMPLING SITE

The 74002/74001 double drive tube was collected in the middle of an irregular, discontinuous deposit of orange glass, at a low area on the southwest rim of Shorty Crater and just east of a large boulder of fractured basalt (Fig. 74-1). The core was taken near the trench, and extended from the Lunar Surface (Muehlberger et al. 73, p. 6-51) to 67.7 cm. At the sampling site, the orange glass deposit occupies a 1 m x 2 m ellipsoidal zone on the surface with the long axis parallel to the crater rim (USGS AFGIT, 1975, p. 14). The extent of the orange area is documented in lunar surface photo AS17-137-20990. Contacts of the orange soil unit and surrounding grey soil are irregular and crenulate, but are roughly vertical, as seen in the trench photos, AS17-173-20987 through 20989. Color zoning within the orange soil exposed in the trench face was also noted by the astronauts to be vertical (voice transcript 05 22 59+), with an outer band of yellowish soil grading inward to orange, and finally reddish soil on the innermost part of the orange glass deposit. (The drive tube was driven straight down, rather than slantwise, to sample the band of orange soil and to avoid the yellow soil.) To the surprise of the astronauts, the soil adhering to the exterior of both the lower and the base of the upper drive tubes was nearly black (voice transcript 05 23 01+), with orange soil discoloring the outside of the upper drive tube to a depth of 25 cm. In addition to the core, samples of the orange soil (74220) and grey soils (74240, 74260) were taken from the Shorty Crater trench.

Heiken et al. (1974) argued that the orange and black soil of 74002/74001 is a sample of stratified material that overlay the subfloor mare basalts; original location of the orange deposits, just above the subfloor basalts, was sketched in an outcrop mosaic by Heiken et al. (1974, p. 1706). Wolfe et al. (1975) interpreted Shorty as an impact crater, with the orange soil being Shorty ejecta. The impact that formed Shorty Crater excavated meter-sized clasts containing these strata and deposited them on the rim where one of the clasts was sampled. This interpretation is sustained here, with the following additions to its support: (1) Patchy areas of colored soil are distributed widely on the southern rim of Shorty Crater. These areas can be recognized by discoloration of overlying surficial materials through mixing with underlying orange and black material, both in close-up view at the trenching site (AS17-137-20990) and in more distant views in Panorama 19 (AS17-137-21007 through - 21013). Distribution of areas of orange, black and grey soil in Pan 19 (AS17-137-21008 through 21011) is sketched in Fig. 1, and occurrence of these colored soils is also indicated on the planimetric site map. (2) Areas of colored soil are approximately the same size as near-by boulders such as the parent of 74255, shown by age dating (Kirsten et al., 1973) to be Shorty Crater ejecta. (3) Bedding is discordant. Orange and black soil in the double drive tube is horizontally stratified, and presumably the rest of the deposit of orange and black soil where the sample was collected is also horizontally stratified, but contacts of orange, yellow, and grey soils are vertical as seen in the trench (voice transcript 05 22 50), photo AS17-137-20990.

In summary, the horizontal stratification of the orange soil, its vertical contacts with grey mare soil, its occurrence in irregular patchy distribution, with color patches the same size as known ejecta blocks in the rim of a known impact crater, is best explained if the core sample came from a clast of orange and black soil deposited in the crater rim by the Shorty event.

The lunar orientation of the core can be inferred (photo documentation failed) from fracture patterns in the trench and in the cores. In trench photographs (e.g. AS17-137-20990) the orange soil appears to be somewhat cohesive, but fractured into polygons which have a prominent set of planar fractures dipping at approximately 60° toward the Shorty crater. Such an internal fracture pattern is seen in stereopair 1 of 74001 x-radiographs. This stereopair, therefore, is interpreted as being oriented radially to the crater, and stereopair 2 is tangential to the crater.

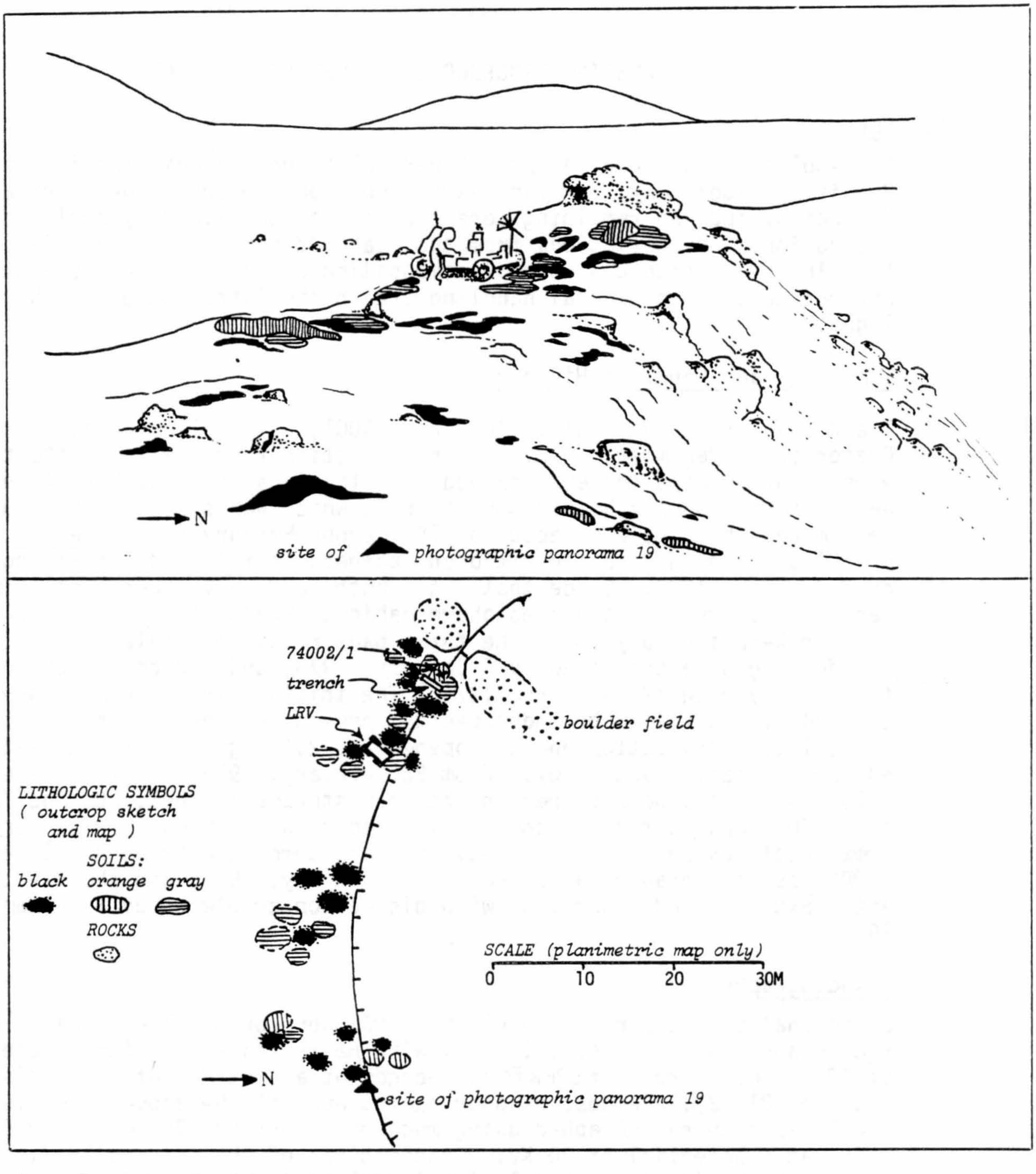

Fig. 1. Sketch of South Rim of Shorty Crater, showing areas of orange, black, and gray soils as seen in PAN 19, and planimetric sketch map (Modified from AFGIT, 1975) depicting distribution of areas of colored soils.

PROCESSING PROCEDURES AND METHODS OF STUDY

1. General

All Apollo cores are given preliminary cleaning and weighing in the Lunar Receiving Laboratory, x-rayed, extracted from the core tube, partially dissected, and the remaining core section is stabilized by peel and impregnation. Any deviations from the standard procedure were related to the fine grain size and unusual composition of the soil in these cores. Further details on general handling are in the introduction to this catalogue.

2. Timelines and Handling History

The double drive tube pair, 74002 and 74001, were collected at Shorty Crater on 12 December, 1972. After extraction from the soil, the tubes were separated and the ends capped. On the lunar surface both tubes were put into Sample Return Container 2, which was sealed in the lunar vacuum and which held a vacuum of 28 microns Mercury (Butler et al. 1973, p. 30) until opened in the nitrogen cabinets in the Lunar Receiving Lab on 3 January, 1973. Since that date, both cores have been kept triple bagged in a dry nitrogen atmosphere cabinet except for a few hours in air for X-radiography (with the three bags remaining sealed). Weighing and dusting were completed by 8 January, 1973, and the core section was first X-rayed on 12 February, 1973. The initial x-radiographs showed that 74001 was filled beyond capacity, preventing the cap from seating properly, so the bottom end was opened and 2.415 gm of soil was extracted for allocation and study. From 22 February, 1973, until 10 December, 1976, both tubes were stored in the core storage cabinet. On the latter date 74001 was re-radiographed, using improved techniques. The core was immediately extruded, and dissections were completed by 30 April, 1972. 74002 was radiographed a second time on 18 May, 1977, and shortly thereafter extruded and dissected, with dissection completed by 1 September, 1977.

3. X-Radiography

Orthogonal stereopairs of 74002 and 74001 were originally prepared by radiography, using a medical x-ray with He-Fe radiation with a potential of 90 Kv and current of 50ma for 5 seconds at a distance of 1 m (this catalogue p. 21-23). Because of poor radiographs at the above conditions, 74001 was also radiographed using much more current (300 ma), for 0.1 sec., at a potential of 80 Kv. Descriptions of the original radiographs appear in the Apollo 17 Sample Catalog (Butler et al. 1973) and Apollo 17 Preliminary Science Report (LSPET, 1973). 74001 yielded the less successful of the original radiographs because the drive tube was largely filled with black, devitrified glass, which is nearly opaque to X-rays. New radiography consisted of 35 min. exposures to multi-spectrum (white) industrial Tungsten X-radiation with a potential of 130 Kv and current of 50 ma. The new radiography used an improved holder that compensated for the curvature of the core tube and provided a flat image.

4. Extrusion

The extruding device failed in the initial attempt to extrude 74001. Because of the high density and internal content of cohesive soil polygons, the designed pressure capacity of the extruder was exceeded. The guide pins that held the extruding screw and attached ram sheared, placing torque on the core holder as well as the extrusion receptacle. This torque fractured the quartz top of the core receptacle, and pieces of quartz contaminated the uppermost part of the core, but otherwise apparently did not disturb the sample. Finally, a device was fabricated that held the ram screw in place well enough to extrude the core, although shavings and pieces of extruder came out of one end of the extrusion device at the same time the core came out of the other end. The pieces of extruder were swept up into a container and transferred out of the cabinet before the core was opened, but unseen labile contaminants from the extruder could have contaminated the cabinet and be in some core samples. Immediately after extrusion, the quartz top was lifted off, the smeared outside surface was scraped off, quartz slivers were picked out, and the prepared surface was photographed.

74002 was extruded in two steps: First, the uppermost 5 mm of core was extruded into a cylindrical receptacle made of 1 mm layers across the axis of the core. The core was then placed vertically and material across the entire diameter of the core was shaved off, 1 mm at a time as the layers of the receptacle were removed. Second, the remaining core was clamped into the extruder and pushed routinely into the dissection receptacle. 74002 was the easiest core to extrude to date, probably because the density did not exceed the capacity of the machine, as 74001 did, because there were no large particles to obstruct free passage of the extruding ram as in 60009 and 60010, and because special care was taken to maintain a straight alignment of the extruding device.

5. Dissection

A. Configuration for each dissection

Both 74002 and 74001 were dissected in three passes along the length of the core, which was placed horizontally on the dissection table. The first and third dissections took place by standard procedures (Lunar Receiving Laboratory Sample Processing Procedure 108) and the second according to the chemically pure mode (in which an effort was made to handle the sample as little as possible, thereby reducing exposure to contamination). Receptacle and layers are illustrated in Fig. 16-17 of the March 1977 update of Lunar Core Catalog. In both the first and third dissections samples were excavated along the length of the core in 5 mm increments, passed through a 1 mm sieve and all particles coarser than 1 mm were identified, measured and weighed. In the "chemically pure" mode of the second dissection, specially cleaned acid-washed tools were used to minimize lead (Pb) contamination. So that there would be a minimum contact between soil and hardware soil was placed directly in acid-washed containers without sieving.

For 74001, the first dissection involved soil under the cover plate, the second involved material under the first 3 side plates (15 mm total thickness) of the receptacle and soil within the last 2 plates (10 mm total thickness) was removed in the 3rd dissection. For 74001, the first dissection removed 7% of the core, the second removed 43% and the third 29%. An illustration of the sideplate configuration is in the 3rd supplement of the Lunar Core Catalog, issued March 1977, Fig. 16-17. For 74002 cover and top sideplate were removed for the first dissection, and then 2 sideplates were removed (10 mm thickness for each pair) for the last two dissections of 74002. In 74002 the first dissection removed 21% of the core, the second and third each removing 29% of the core. In both cores, a remainder of 21% was left for peeling and impregnation.

Figs. 16 through 27 document the subsample numbers and locations of all splits removed during standard dissection of 74001 and 74002. Table I lists all photographs taken during processing of these cores.

B. Sample handling procedures during dissection

Standard 5 mm dissection intervals along the core were used, and a detailed description of each interval in place was followed by its extraction, sieving, and binocular examination. However, because of the fine grain size (only 3 coarse particles were retained on the 1 mm sieve in all of 74001) and lack of obvious texture changes, emphasis was placed on the study of the visible coarse fraction on the surface planed off during the previous dissection pass. Maximum grain size was recorded, types and color of droplets noted where possible. Next 2 or 3, observational 5 mm^2 areas were marked off on the surface of each interval and all visible grains in each area were classified according to their being single, double, or compound droplets. This procedure was designed to test for changes in grain type and to look for incipient marbling that might be missed because of uniform color and apparently uniform texture. If two observational areas were statistically different in each interval, one would suspect marbling. This procedure has the limitations: (1) Only the coarsest material was examined, because particles under 50 microns were too small to see the dissecting microscope, and (2) vitreous glass is disproportionately represented because black, devitrified glass shows up poorly in reflected light and is likely to be missed. During dissection, degree of cohesiveness and size of fracture polygons in each unit was noted.

The lowest 22 cm of 74002 was as fine grained as 74001 and was dissected in the same manner. Above 10 cm, cm-size clasts of orange soil could be recognized in the core, but the clasts could not be extracted as separate entities between 10 and 5.5 cm. Small amounts of orange soil could be removed, but the clasts interfingered too closely with the surrounding soil for separate extraction. On the other hand, clasts of orange and dark soil, agglutinates, and mare basalts and breccia fragments occurred in the coarse fraction between 5.5 cm and the top of the core; these are reported as "coarse fraction" in the dissection charts, and should be studied as detrital components as well as the orange and black glass droplets, fragments of droplets, and mineral grains.

The fineness of the soil, however, made it necessary to prepare grain mounts from 1 mg samples taken at strategic locations through the core in order to obtain quantitative date on grain size and composition.

Table I.

LIST OF PHOTOGRAPHS

Topic of illustration	74001	74002		
Pre-extrusion, top 5 mm		S-77-27496-27510		
Coarse fraction top 5 mm		S-77-27640-27644		
Post-extrusion	S-77-20775-20778 & 20968	S-77-28106-28113		
Pre-dissection 1	S-77-20779-20788	S-77-28096-28105(poor color) S-77-29911-29920(better color)		
Post-dissection 1	S-77-21977-21981	S-77-28126-28135		
Post-dissection 2	S-77-23404-23413	S-77-28462-28472		
Post dissection 3	S-77-26923,26926,26928 and 26858	S-77-28491-28500		
Peel	S-77-26921-26934(partial set) and 26859-26861(rest of set)			
Impregnation	S-77-26957,26958			
Dissection clasts and structures			Interval	
		S-77-28069	(30.0-29.5 cm)	
		S-77-28068	(25.0-24.5 cm)	
		S-77-28306	(22.5-22.0 cm)	
		S-77-28305	(21.0-20.5 cm)	
		S-77-28304	(19.0-18.5 cm)	
		S-77-28307	(17.0-16.5 cm)	
		S-77-28181 28184	(14.0-13.5 cm)	
		S-77-28183 28179 28180	(8.0-7.0 cm)	
Coarse fraction in detrital interval at top of 74002		Photo No.	Interval	Sample
		S-77-28527	1.0-0.5	-,2071
		S-77-28528	1.0-0.5	-,2071
		S-77-28172	1.0-0.5	-,88
		S-77-28174	1.5-1.0	-,88
		S-77-28525	1.5-1.0	-,2069
		S-77-28526	1.5-1.0	-,2061
		S-77-28178	2.0-1.5	-,85
		S-77-28523	2.0-1.5	-,2067
		S-77-28524	2.0-1.5	-,2067
		S-77-28175	2.5-2.0	-,85
		S-77-28521	2.5-2.0	-,2065
		S-77-28522	2.5-2.0	-,2065
		S-77-28176	3.0-2.5	-,83
		S-77-28519	3.5-2.5	-,2063
		S-77-28520	3.5-2.5	-,2063
		S-77-28177	3.5-3.0	-,81
		S-77-28173	4.0-3.5	-,79
		S-77-28517	4.5-3.5	-,2060
		S-77-28518	4.5-3.5	-,2060
		S-77-28516	5.5-4.5	-,2057
		S-77-28515	5.5-4.5	-,2057

C. Preliminary examination of grain mounts

Following the first dissection, grain mounts were prepared and studied to obtain a measure of compositional and textural variations that was more accurate than measurements under the dissecting microscope. Ten such Preliminary Examination samples were selected as follows, from each core:

Table II. Data on grain mounts from drive tubes 74002/74001.

Sample	Interval below top of core (cm)	Rationale for sampling
74002		
- ,99	2.0- 2.5	Characterize upper part of section, in which agglutinates and rock fragments occur.
- ,98	8.0- 8.5	Evaluate whether dark soil with clasts, between 10 and 5.5 cm, is fallback breccia associated with Shorty Crater, or secondarily reworked and gardened material.
-, 97	12.0-12.5	Characterize the most pure orange soil in core.
-, 96	14.0-14.5	Compare moderately light, massive soil to orange soil, and to friable, moderately light soil.
-, 95	15.5-16.0	Characterize and compare moderately light soil to darker soil.
-, 94	17.0-17.5	Characterize moderately dark soil that is friable, compare it to similar, but massive soil, and to lighter soil that is also friable.
-, 93	19.0-19.5	Characterize moderately dark soil that is massive.
-, 92	21.5-22.0	Compare upper part of dark, friable zone to lower part of same zone to see if internal changes within one zone are more or less than changes between zones.
-, 91	24.0-24.5	Characterize dark, friable soil, compare it to dark, massive soil.
-, 90	26.5-27.0	Characterize massive, dark soil from base of core.
74001		
-,374	1.5- 2.0	Characterize upper part of friable interval (Major unit 3).
-,375	6.0- 6.5	Compare upper and lower parts of friable interval.
-,376	9.0- 9.5	Characterize hard, massive zone (Major unit 2).
-,377	13.5-14.0	Compare thin, crumbly lamina in hard, massive zone to more cohesive portions of same major unit.
-,378	14.5-15.0	Text for small-scale variation between massive and crumbly parts of major unit 2. This sample is relatively hard and cohesive.
-,379	16.5-17.0	Characterize lower part of massive zone (Major unit 2).
-,380	20.5-21.0	Characterize lower friable zone, and search for internal variations within this predominantly homogeneous unit.
-,381	23.0-23.5	" " " "
-,382	27.0-27.5	" " " "
-,383	32.0-32.5	" " " "

Data collected during study of grain mounts encompasses size distribution, composition, and particle morphology (Tables V, VI, VII). In determining grain size, point-count passes were made across each slide until six passes were completed or 500-points were counted. Data were not collected where multiple grains obscured the others. Grains were assigned to the following size classes to be comparable to data of other workers: < 0.01 mm, 0.01 - 0.06 mm, 0.06 - 0.12 mm, 0.12 - 0.25 mm, 0.25 - 0.5 mm, and 0.5 - 1.0 mm.

Compositional parameters quantified for the 3 size fractions in the range 0.01 - 0.06, 0.06 - 0.12 and 0.12 - 0.25 mm include orange glass, black 'glass", pyroxene, olivine and plagioclase. Because grain mounts were not ground to a uniform thickness to reduce loss of material, mineral grains could not be identified using standard relief and birefringence criteria; but were recognized on the basis of cleavage, internal fracture, relative birefringence, and twinning. Grains that were strongly twinned and which showed well-defined cleavage were classified as pyroxene whereas untwinned grains with high birefringence and irregular internal fracture were classified as olivine. Some of the identifications may be erroneous, but changes in characters are internally consistent through the cores and correspond to other major changes in the cores.

Characterization of the morphologies of the orange and black particles follows the categories of Heiken et al. (1977) and includes complete and broken spheres, complete and broken ovoids, indeterminate fractured particles and compound particles. Because of limited sample particle numbers in the 1 mg grain mounts, it was not always possible to find 500 objects in a grain category, but as many points as possible were counted. For the size classes between 0.01 and 0.25 mm, variations of morphology of individual components were quantified as follows: orange glass, abundance of entire and broken spheres, ovoid droplets, compound particles and indeterminate broken fragments. Similar data were collected for black (devitrified) glass, except that broken particles rarely showed sharp fractures because they were recrystallized or secondarily coated with tiny glass droplets, and the broken particles were accordingly classified into a single category. Crystallized, non-glassy grains were abundant in the grain mounts, and were classified to principal mineralogy (pyroxene or olivine) and genetically identified as xenoliths or xenocrysts (untwinned angular grains with smooth edges and no reaction rims) and droplet pseudomorphs (crystallized glass droplets that show external form of droplets, but are internally crystallized, showing a fine internal structure and no reaction rims). Composition of pseudomorphs was related to pyroxene (strongly twinned with well-defined cleavage) or olivine (apparently not twinned, with irregular, internal fracture).

RESULTS

1. X-radiograph stratigraphy

Descriptions of the new x-radiographs appear in Figs. 2 and 3. Although description was still hindered by the opacity of the samples, much more information could be obtained on internal massiveness, size and type of internal fracture polygons and internal structure. On the

Fig. 2 RE-RADIOGRAPH OF DRIVE TUBE 74002

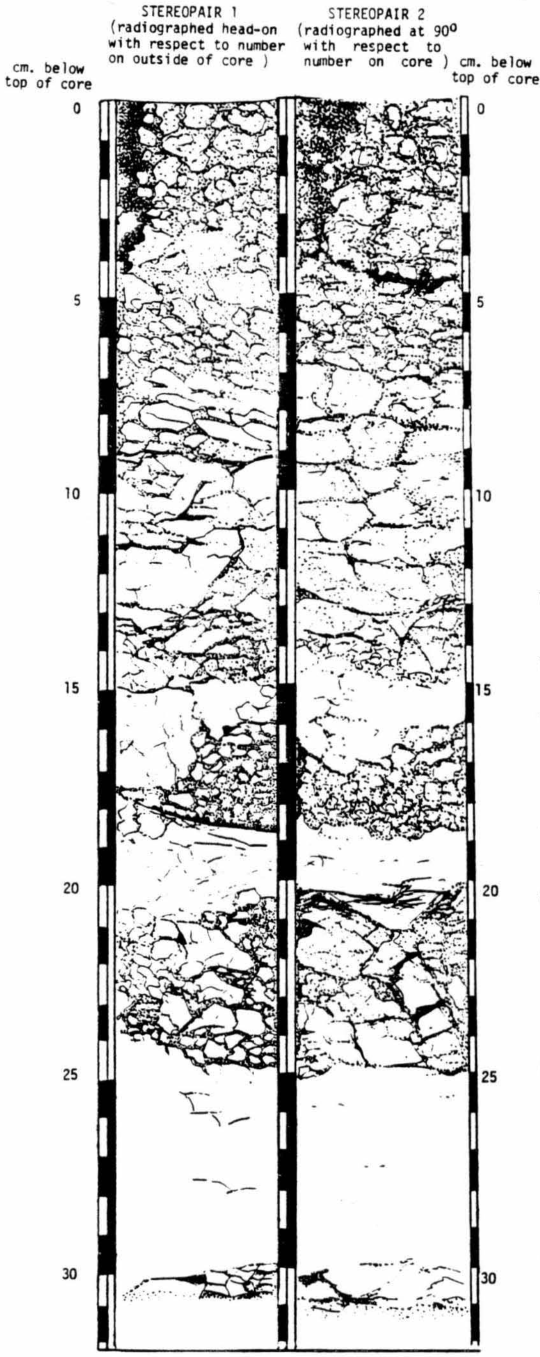

Interval	UNIT	Boundary	Description of Unit
0.0 - 4.5 cm	X		Loosely compacted, marbled interval with clasts 65% of total, clasts are equant, subrounded, irregular to lumpy-margined, 2 cm to 1 mm in size, with clasts being 2 cm at the base of the unit, but averaging 3 mm at the top.
4.5 - 7.0 cm	IX	partially void, irregular	Interval with medium-scale marbling, with 75% clasts, 25% matrix, with elongate to irregular clasts ranging from 2 mm to 1.5 cm , progressively increasing in size toward the top of the unit.
7.0 - 13.0 cm	VIII	transitional over 1/2 cm.	Coarsely marbled to shattered interval, 90% coarse, 10% matrix or interstital material; internal polygons are 1 - 3 cm in diameter, are evenly-sized with subrounded edges, and in this way resemble clasts, but polygons are stacked as blocks, not randomly aligned as in a marbled stratum, and many polygons show similar configuration on opposite sides of fractures.
13.0 - 14.5 cm	VII	transitional	Shattered to marbled interval, 80% coarse particles, 20% matrix or interstital material; coarse particles are mostly rhombohedral fragments with semi-planar sides, 2 cm to 5 mm in diameter; some conchoidal, cross-cutting fractures present.
14.5 - 17.5 cm	VI	indistinct, irregular	Massive interval, moderately opaque, with common, irregularly rectangular fractures and intersecting sets of fractures.
17.5 - 18.5 cm	V	distinct, irregular	Finely marbled interval, consisting of 65% clasts, 35% matrix, clasts are fairly evenly-sized 5 mm equant to elongate, irregular lumpy, randomly-aligned particles.
18.5 - 20.5 cm	IV	distinct, semi-planar surface	Massive interval, moderately opaque, with numerous 1 - 2 cm thin, horizontally-aligned, planar to conchoidal fractures.
20.5 - 25.0 cm	III	distinct, irregular	Marbled interval, with 75% clasts, 25% matrix; clasts are poorly sorted, ranging from 2.5 cm to 2 mm., larger clasts are planar-faced polyhedrons, but smaller clasts are irregularly subrounded lumpy objects.
25.0 - 30.5 cm	II	distinct, but in stereopair 1 seems to show some plucking from top of underlying unit	Massive interval, moderately opaque, with scattered cm - length, horizontal, planar to conchoidal fractures.
30.5 - 32.5 cm	I	transitional	Shattered interval, moderately opaque, as overlying unit, but with numerous 1 - 4 cm straight to conchoidal fractures. Unit is interpreted to be a continuation of Unit II, fractured and disrupted during handling.

Fig. 3j

RE-RADIOGRAPH OF DRIVE TUBE 74001

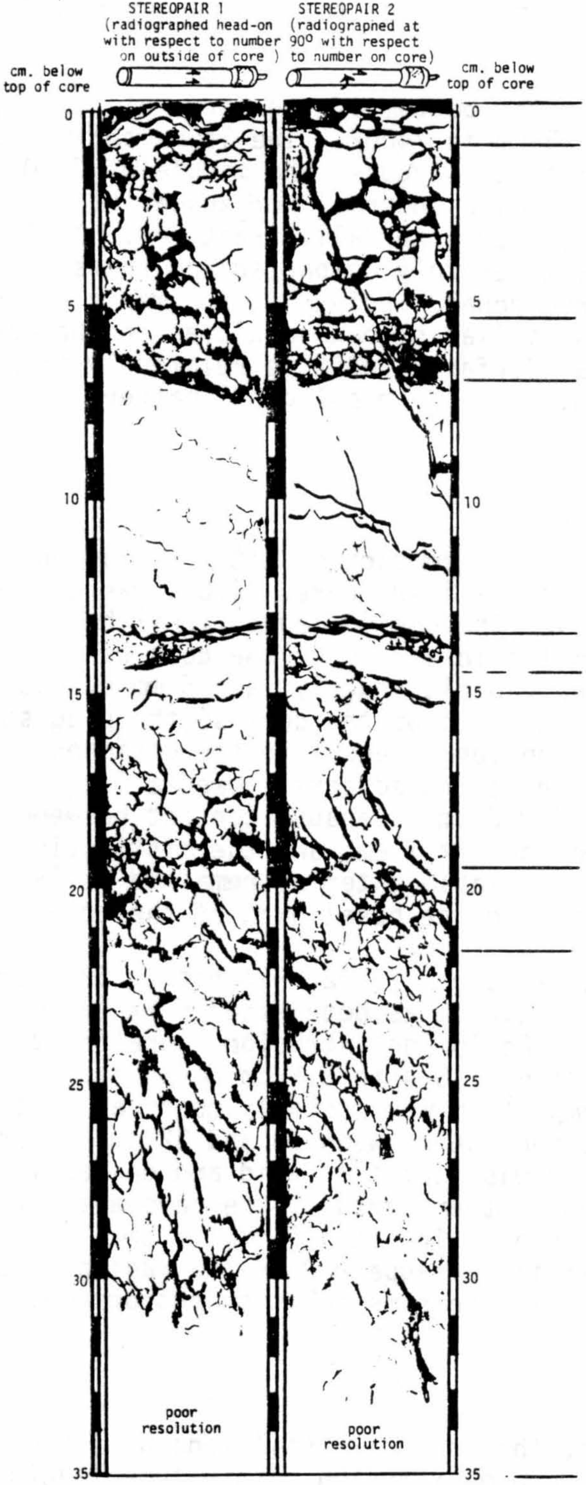

Interval Unit	Boundary	Description of Unit
-0.3 - 1.0 cm IX		Partially void with equant clods or clasts averaging slightly less than 1 cm in diameter, and with subrounded edges. Transverse fractures predominate.
	transition	
1.0 - 5.5 cm VIII		Relatively massive unit with approximately 75% clasts and 25% matrix. Clasts average 2 cm in diameter, and range is size down to 4 mm. The clasts are mostly equant, with relatively straight edges. A major inclined fracture cuts this unit, as seen in stereopair 2.
	indistinct transition	
5.5 - 7.0 cm VII		Finely clastic-appearing unit with a 50-50 clast to matrix ratio, with 2 - 8mm relatively equant clasts evenly distributed through the unit. A major fracture system appears in stereopair 2, inclined at approximately 60° to the horizontal, and extending from 1 cm. in the upper unit to a depth of 10 cm. in unit VI.
	sharp, planar, inclined contact	
7.0 - 12.5 cm VI		Massive unit with dense internal appearance, with no clods or clasts internally, but a transverse fracture system at 13.5 cm.
	distinct bowl-shaped contact, convex downward	
13.5 - 14.5 cm V		Finely granular, thin unit with approximately 40% mm-sized, equant, sorted, subrounded granules.
	distinct, curving contact, convex downward	
14.5 - 15.0 cm IV		Thin but opaque and dense unit, with no well-defined internal fractures. Similar to VII, but thinner.
	distinct curving contact, convex downward	
15.0 - 19.5 cm III		Fracture polygon unit, with polygons of sizes varying from 5mm to 4 cm, with 60% of the unit made of the largest size polygons, the remainder of 0.5 to 1 cm. polygons. Largest polygons appear to be tabular to wedge-shaped in stereopair 2, and are bounded by nearly planar fractures inclined at approximately 60° to the vertical, and as long as the polygons. Smaller polygons are equant, with irregular edges.
	transition	
19.5 - 21.5 cm II		Cloddy interval, with 30% matrix, 70% clods ranging from 3mm to 2 cm, and with an even distribution of all sizes indicating poor sorting. Although 25% of clods, by area, have straight, fractured edges and appear to have wedge shape, most clods are equant with highly irregular edges.
	indistinct but planar contact	
21.5 cm I	to base of core	(The base of the drive tube has a thick metal bit which obscures internal features in the lowest 3 cm. Examination of the lowest part of the core during preliminary examination indicated that there was 2 to 3 mm of soil protruding out of the bottom end of the drive tube, and that the core was more than 100% full, as a result.) Interval with large inclined fracture polygons, most of which are 1 - 2 cm long, half as wide and thick. Sizes of polygons vary from double to half the above. Most polygons are inclined approximately 60° to the horizontal in stereo 1, and have relatively sharp, planar boundaries.

NOTE: The whole of core 74001 is relatively opaque and resistant to X-rays, and is interpreted to be composed entirely of the fine-grained black devitrified glass that was reported by Astronauts Cernan and Schmitt to occur at the top and bottom of the core (Bailey and Ulrich, 1975, p. 154). Core 74002 showed alternating layers of radiographically opaque and transparent material, with the transparent material occurring toward the lunar surface, at the top of the core. Vitreous glass passes X-rays whereas the crystal planes in the devitrified, crystalline glass scatter the X-rays, making it radiographically opaque. Therefore it is believed that the orange glass is confined to the radiographically transparent zones in 74002.

Within 74001, there are no density or opacity changes suggestive of rock fragments; instead, most changes are seen as obliquely intersecting zones of slightly lower opacity, suggestive of internal fractures. However, at the top of the cores, there are some clods of dark glass. The clods can be distinguished from fracture polygons by being relatively rounded, with edges which fade out rather than terminate abruptly. Furthermore, adjoining edges of fracture polygons fit together whereas edges of clasts are discordant. Sizes of internal polygons varies throughout the core, enabling identification of discrete zones which are interpreted herein as being parts of more extensive strata.

basis of these parameters, it was possible to distinguish nine units in 74001 and ten in 74002.

Massive units predominate from the bottom of the core, all through the lower tube, 74001, and up to 25 cm in 74002. The lower part of 74001 shows indistinct cm-sized fracture polygons, the middle of 74001 and the lower part of 74002 are massive with internal horizontal stratification, and the top of 74001 is massive but internally fractured. In 74002 from 25 cm up to 7 cm, the core is moderately compacted and shows an alternation of massive and fractured zones. Polygonal fragments in some fractured zones can be matched to similar-shaped vacuities in the massive zones. From 7 cm to the Lunar Surface, 74002 is relatively transparent and de-densified, showing a 0.5 cm - 2 cm polygonal pattern.

2. Depth effects

A. Compaction Due to Extrusion

Both cores showed a small amount of compaction after extrusion was completed. The original length of the lower core, 74001, was apparently 35.7 cm, approximately 8 mm over the design capacity of the drive tube. The 3 mm of soil bulging from the lower end of the core was scraped off in 1973, (74001, 2 & 3) so the cap fit snuggly, and 5 mm of excess soil (74001,21) was excavated from the top of the core so the plug seated properly leaving a pre-extrusion length equal to the designed capacity of the drive tube; 34.9 cm. The extruded core showed a length of 34.3 cm, indicating a compaction of 0.6 cm. Because contact between the massive and crumbly units remained at 7 cm, and the distinctive transition between semi-friable and friable material remained at 19 cm compaction apparently was confined to the basal part of the core.

The original length of the upper core, 74002, was either 32.5 cm as measured on X-radiographs, or 32.4 cm as determined from hardware measurements prior to extrusion. Following extrusion, core length was 32.0 cm, indicating a compaction of 0.4 to 0.5 cm, depending on which original length is used. Compaction was probably confined to the lower end of the core, because the section between 30 and 32 cm appears tightly compacted after extrusion, but was partially void and de-densified before extrusion in the X-radiograph. Other parts of the core are uncompacted, as evidenced by non-disruption of voids at 1-5 cm, 16 cm, 18 cm, and 20-22 cm. These voids appear in stereopair 2 of the radiographs, taken shortly before extrusion, and in the same position photographs, taken shortly after extrusion.

B. Sample Depth Convention

As best as can be determined, the original total length of the core was 68.1 cm, including in 74001, a pre-extrusion within-tube length of 34.9 cm, and 0.8 cm of removed material, and in 74002, a 32.4 cm pre-extrusion length. Although location of compacted intervals can be inferred by comparing the extruded soil column to X-radiographs, it is not possible to determine precisely the exact degree and amount of compaction everywhere in the core. Hence, depth values on dissection diagrams and related sections are given in post-extrusion figures, which can be directly related to scale intervals shown in photographs of the cores in the dissecting table, and which are used to account for sample position in the LCL (Lunar Curatorial Laboratory) Sample Inventory. Using post-extrusion figures, 74002 is 32.0 cm long, the removed material from the top of 74001 is 0.5 cm long, the dissected core 74001 is 34.3 cm long, and the 0.3 cm of material removed from the base of 74001 gives a post-extrusion total soil column length of 67.1 cm. Depth in each core, as entered in the LCL inventory, starts at the top of the soil in the dissection receptacle. Calculations of depth below Lunar surface in 74001 should add the 0.5 cm of soil removed before extrusion to the length of 74002, to get the soil column above the top of 74001.

3. Stratigraphy from Binocular Microscope Observation

A. Introduction

Some changes in the exposed core could be related to changes seen in X-radiograph but other parameters showed no correlation between X-radiographs and parameters seen under the binocular microscope. During dissection, it was found that few > 1 mm particles occurred below 5.5 cm, and all appeared to be tiny particles of orange glass, black devitrified glass or mineral grains. Abundances of these were estimated under the binocular microscope, under the section "continuous trends". Many coarse particles were recovered from the interval between 5.5 cm and the Lunar Surface; occurrence of these is documented next, under "Properties of the upper 5.5 cm of 74002."

B. Continuous Trends

The limited data that could be taken during dissection are listed in Table III; the data were verified by comparison to grain mounts at the same intervals. Table III includes estimated percent coarse (larger than approximately 0.1 mm) droplets, maximum droplet size, maximum common droplet size, and percent of droplets which are orange and black. Of these criteria, changes in percent coarse (Fig. 74-16) as well as in maximum droplet size, in conjunction with structural data, were used to define the boundaries of the stratigraphic units and provide the only continuous data over the entire core. Changes in the proportions of orange and black glasses are as likely to occur within units as at unit boundaries.

C. Comparison of Grain Mount and Dissection Data

During dissection, attempts were made to estimate size-distributions of the coarser particles, and to evaluate abundance of orange and black droplets larger than 0.1 mm (practical limit of visibility under the dissection microscope), and to evaluate abundance of single and compound grains. Table 1 shows size and composition estimates from the grain mounts, and for equivalent dissection intervals. Dissection 1 was performed first, then the grain mounts were examined, and dissection 3 was conducted with grain mount data on hand so that adjustments could

Table III. Continuous Trends, Cores 74001 and 74002

	74001				74002			
Sample Interval (LCL Inventory)	% Coarse	Max Size *1	Max Abundant	% Orange *2	% Coarse	Max Size *1	Max Abundant	% orange *2
	Top of 74001				Top of 74002 removed earlier			
010-05	5	.5 -.25	.25	15-20	5	.25-.12	.12	72
015-10	5	.5 -.25	.25	15-20	5	.25-.12	.12	72
020-15	5	.5 -.25	.25	15-20	5	.5 -.25	.18	66
025-20	5	.25-.12	.12	15-20	5	.5 -.25	.25	66
030-25	3	.25-.12	.12	15-20	5	.5 -.25	.25	72
035-30	2	.25-.12	.12	15-20	8	.5 -.25	.25	72
040-35	2	.25-.12	.12	15-20	8	.5 -.25	.25	70
045-40	5	.25	.25	15-20	12	.5 -.25	.25	72
050-45	5	.25	.25	15-20	10	.25-±	.25	70
055-50	4	.25	.25	15-20	10	.5 -.25	.25	70
060-55	4	.25	.25	15-20	10	.25-±	.25	68
065-60	2	.25-.12	.12	15-20	10	.25-±	.25	66
070-65	2	.25-.12	.12	15-20	10	.25-±	.25	66
075-70	5	.50-.25	.25	5-10	10	.5 -.25	.25	68
080-75	5	.50-.25	.25	5-10	10	.5 -.25	.18	66
085-80	5	.50-.25	.25	5-10	8	.25-.12	.18	72
090-85	5	.50-.25	.25	5-10	5	.25-±	.25	74
095-90	4	.50-.25	.25	5-10	6	.5 -.25	.25	86
100-95	3	.50-.25	.25	5-10	6	.25-±	.18	88
105-00	5	.50-.25	.25	5-10	6	.5 -.25	.18	78
110-05	5	.50-.25	.25	5-10	7	.5 -.25	.25	92
115-10	5	.50-.25	.25	5-10	8	.25-±	.25	84
120-15	5	.50-.25	.25	5-10	7	.5 -.25	.25	90
125-20	2	.25	.25	5-10	6	.5 -.25	.25	88
130-25	2	.25	.25	5-10	7	.25-±	.25	66
135-30	3	.25	.25	5-10	6	.25-.12	.25	62
140-35	3	.25	.25	5-10	6	.25-.12	.18	66
145-40	3	.5 -.25	.25	5-10	8	.25-.12	.18	46
150-45	3	.5 -.25	.25	5-10	8	.25-.12	.18	50
155-50	3	.5 -.25	.25	5-10	7	.5 -.25	.18	48
160-55	3	.25-.12	.12	5-10	7	.5 -.25	.18	46
165-60	3	.25-.12	.12	5-10	7	.5 -.25	.25	44
170-65	3	.25-.12	.12	incr	7	.5 -.25	.18	44
175-70	3	.5 -.25	.25	to	6	.5 -.25	.25	36
180-75	3	.5 -.25	.25	20%	4	.5 -.25	.25	32
185-80	3	.5 -.25	.25	20	4	.5 -.25	.18	26
190-85	3	.5 -.25	.25	20	5	.25-±	.25	25
195-90	3	.5 -.25	.25	20	6	.25-±	.25	25
200-95	3	.5 -.25	.25	20	6	.25-±	.25	26
205-00	3	.25-.12	.12	20	6	.25-±	.18	18
210-05	3	.25-.12	.12	20	10	.5 -.25	.18	18
215-10	3	.25-.12	.12	15-20	10	.5 -.25	.18	26
220-15	2	.25-.12	.12	10-15	10	.5 -.25	.18	26
225-20	2	.25-.12	.12	5-10	9	.25-.12	.18	32
230-25	3	.25-.12	.12	5-10	6	.25-.12	.25	18
235-30	5	.25-.12	.12	5-10	6	.25-.12	.12	12
240-35	4	.25-.12	.12	5-10	5	.25-.12	.18	18
245-40	2	.25-.12	.12	5-10	4	.5 -.25	.18	23
250-45	2	.25-.12	.12	5-10	5	.4 -.25	.18	23
255-50	6	.5 -.25	.25	5-10	4	.5 -.25	.12	23
260-55	5	.5 -.25	.25	5-10	4	.5 -.25	.12	30
265-60	4	.25	.25	5-10	5	.5 -.25	.18	24
270-65	4	.25	.25	5-10	4	.5 -.25	.18	26
275-70	3	.5 -.25	.12	5-10	5	.5 -.25	.18	22
280-75	2	.25-.12	.25	5-10	6	.25-.12	.18	23
285-80	2	.5 -.25	.12	5-10	7	.25-.12	.18	19
290-85	2	.5 -.12	.12	5-10	5	.5 -.25	.18	19
295-90	2	.25-.12	.12	5-10	8	.5 -.25	.18	18
300-95	5	.25-.12	.12	5-10	6	.25-.12	.18	17
305-00	5	.25-.12	.12	5-10	6	.25-.12	.12	15
310-05	5	.5 -.25	.25	5-10	6	.25-.12	.12	16
315-10	5	.5 -.12	.12	5-10	6	.25-.12	.18	14
320-15	4	.25-.12	.12	5-10	6	.25-.12	.18	14
325-20	3	.25-.12	.12	5-10	Base of 74002			
330-25	3	.25-.12	.12	5-10				
335-30	4	.5 -.12	.12	5-10				
340-35	4	.5 -.12	.12	5-10				
345-40	4	.25-.12	.12	5-10				

Base of double core

*1 Max. size indicates approximate size of largest particles in 5 mm interval
Max. abundant indicates approximate size of largest abundant particles in 5 mm interval
*2 % orange is percentage of 150 droplets/interval visually estimated to be orange. The remainder appeared to be black.

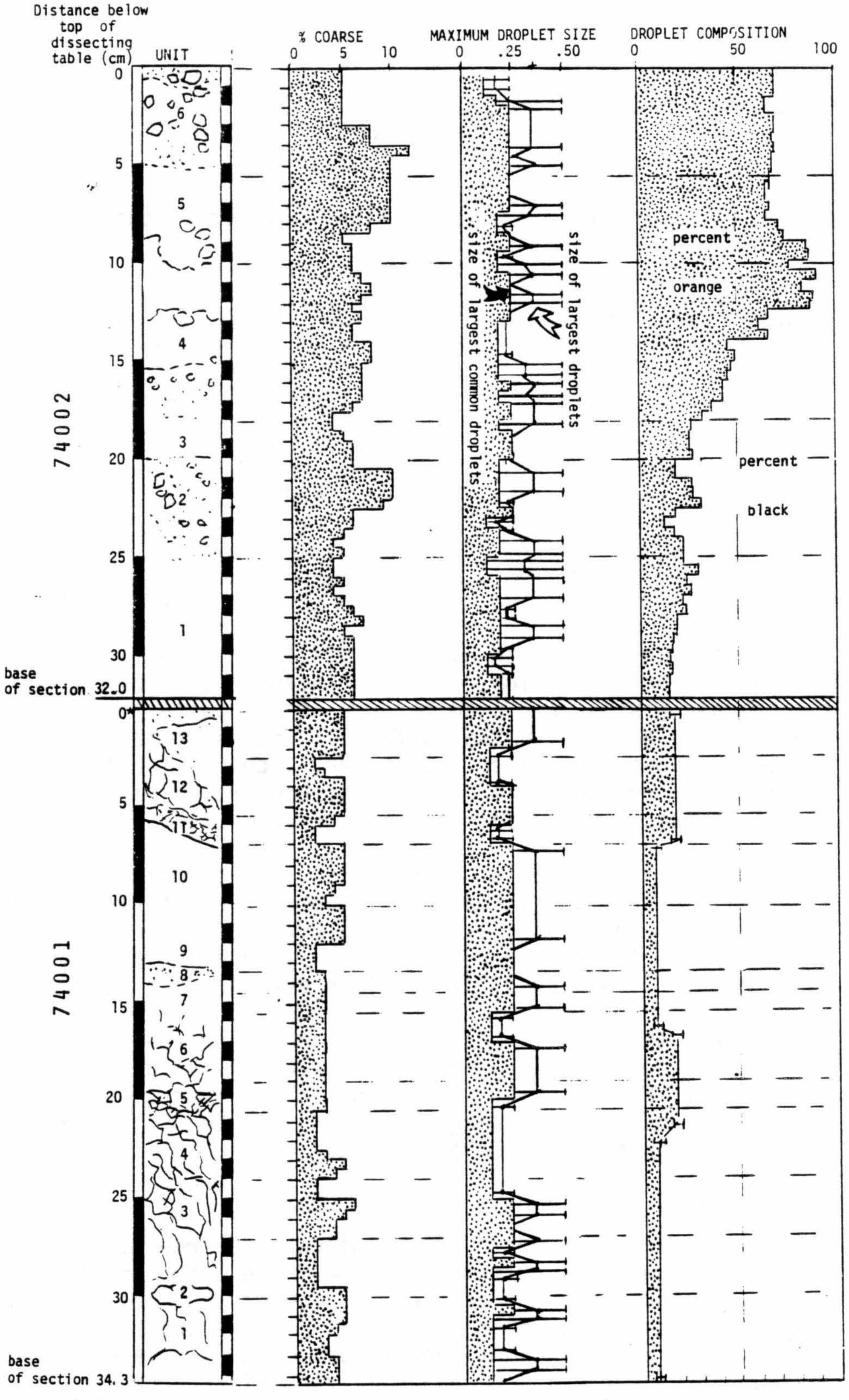

Fig. 4. Continuous trends, drive tubes 74002/1. Data are from table III. "% coarse" is abundance of particles 0.1 mm, and size range of largest common particles is indicated by error bars under "maximum droplet size".

be made to visual estimates.

Table IV. Comparison of grain mount and dissection data on 74002 petrography

	DISSECTION 1					GRAIN MOUNTS					DISSECTION 3				
		% in size class (mm)					% in size class (mm)					% in size class (mm)			
Interval	Sample No.	0.5-.25	.25-.12	percent orange	percent compound	Grain Mount No.	0.5-.25	.25-.12	percent orange	percent compound	Sample No.	0.5-.25	.25-.12	percent orange	percent compound
2.0 -2.5	-,84	Tr.	7-10%	71%	19%	-,99	0.8%	1.6%	56%	30%	-,2065	Tr.	10-12%	66%	10%
8.0 -8.5	-,68	3%	7-10%	88%	14%	-,98	0.4%	3.6%	53%	35%	-,2049	Tr-1%	10-15%	72%	10%
12.0-12.5	-,59	3-5%	7-10%	92%	12%	-,97	1.8%	4.6%	70%	25%	-,2040	Tr.	10-15%	88%	Tr.
14.0-14.5	-,53	3-5%	7-10%	93%	18%	-,96	1.4%	5.0%	53%	40%	-,2036	Tr.	7-10%	46%	10%
15.5-16.0	-,50	5%	7-10%	92%	19%	-,95	0.8%	3.4%	43%	40%	-,2033	Tr.	12-15%	46%	10%
17.0-17.5	-,47	3-5%	7-10%	90%	24%	-,94	1.2%	7.0%	44%	40%	-,2030	Tr.	10-12%	36%	50%
19.0-19.5	-,43	2-3%	7-10%	78%	28%	-,93	0.8%	1.4%	32%	50%	-,2026	Tr.	7-10%	25%	50%
21.5-22.0	-,38	5%	7-10%	75%	23%	-,92	0.4%	3.6%	25%	60%	-,2021	1-2%	7-10%	32%	65%
24.0-24.5	-,33	Tr.	5 -7%	77%	28%	-,91	indet., poor slide		18%	75%	-,2016	1-2%	7-10%	5-10%	95%
26.5-27.0	-,28	2%	5%	67%	23%	-,90	0.6%	2.2%	7%	85%	-,2011	1-2%	7-10%	5-10%	95%

As can be seen on the table, it is difficult to obtain meaningful size estimates from dissection, probably because fine grains mask some of the coarser grains, and also because other coarse grains which shed dust appear to be perched on the surface of the dissected core, giving them an apparent high abundance. In general, coarser-grained intervals were consistently recognized and distinguished from finer-grained intervals, both in dissection and in observing grain mounts.

Without prior knowledge of composition, the abundance of orange glass, as seen in dissection 1, was consistently overestimated, and the abundance of compound grains was greatly underestimated. Binocular estimates of abundances for the third dissection were calibrated with the grain mount data. It was possible to differentiate with confidence, the orangish but dull, metallic-appearing grains originally classified as orange from the bright, shiny grains that were really orange. General trends were consistently recognized, even if the data were quantitatively inaccurate. Furthermore, it was possible during dissection to detect both rapid and gradual changes over the length of the cores, even if it was not possible to obtain quantitative data.

D. Comparison of Binocular and X-ray Data

A study of X-radiographs of 74001 discerned three major units, the lowest extending between 19 cm and the base of the core, the next between 7 and 19 cm, and the uppermost between the top of the core and 7 cm. X-radiography also revealed internal changes in fracture pattern within the major units; these changes were regarded as unit-level changes. During dissection, major units were easily recognized because the upper and lower major units were internally fractured and readily distinguished from the middle major unit which was massive and cohesive. In the massive middle part of the section, X-ray units were recognized and defined petrographically, but it was not possible to recognize petrographic units in the X-radiograph of the upper and lower major units. The grain size variations that enabled petrographic definition of the units could not be seen in the X-radiograph.

Similarly, in 74002, X-radiograph units II, III, IV, V and X, identified in part on major changes in internal fracture pattern, were identified by fracture pattern during dissection, but units between 5 and 20 cm, identified in dissection on petrographic compositional changes, were unrecognizable in X-radiograph.

In general, units that had internal fracture characteristics as an important defining property were recognized in X-radiograph as well as in dissection. Units based on petrographic changes were consistently not identified in X-radiograph.

4. Internal structures and variation across the core

74001 was nearly uniformly dark, and units showed little contrast between each other, with the most obvious differences being relatively subtle changes in cohesiveness and abundance of large droplets. No well-defined unit boundaries could be seen during dissection, but grain-size and cohesiveness changes seen on one side of the core were found at the same depth position on the other side. With such unclear data, the best one can do is infer that stratal boundaries persist relatively straight across 74001, and that strata are relatively flat-lying. X-radiographs show some planar surfaces that are roughly horizontal, but it was not certain during dissection that these were stratal boundaries or shear zones.

In contrast to the unclear boundaries of 74001, distinct orange and black color changes are easily seen in 74002, especially in the upper part of the core. Below 10 cm, most color boundaries at 13, 17, 20 and 25 cm were broadly irregular but persisted across the core in a manner that suggested slightly disturbed but relatively flat-lying strata. Above 10 cm, stratal character changes sharply, as illustrated in Fig. 05. Between 10 and 5.5 cm are numerous cm-sized, crenulate, vertically-aligned very friable orange clasts in a dark matrix. Although individual clasts are relatively small, the general characteristics of the unit persist across the core in the same part of the section. At approximately 5.5 cm, there is a textural change marked by an irregular but relatively horizontal boundary. Above this boundary, most elongate particles are horizontally aligned, rather than vertical, and rounded clasts take the place of the crenulate clasts that were so abundant between 5.5 and 10 cm. This general structural configuration continues to the top of the core, with a maximum in orange clasts between 2 and 3 cm depth.

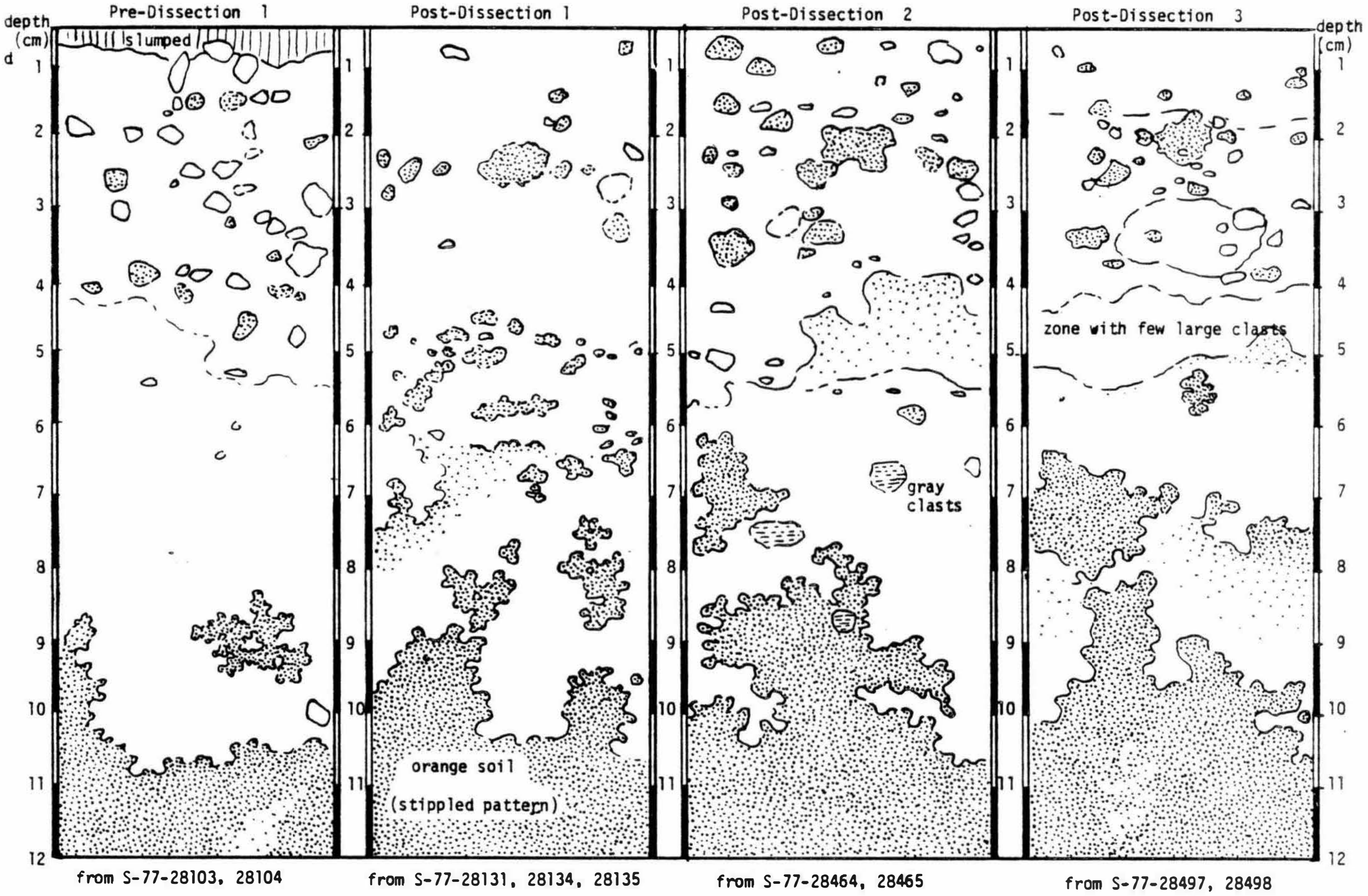

Fig. 5. Internal structures in the upper part of 74002

5. Stratigraphy from study of Grain Mounts

A. Textural Changes

Variation in grain size through the cores appears in Fig. 6. Although there are no spectacular changes, the lowest quantity of very fine material occurs at 17 cm in 74002. From there, the mean size decreases upward to the lunar surface and downward to the bottom of the core. Quantitative sieve data may change these results.

B. Compositional Changes

In contrast to the relative uniformity in size, there are major variations in composition throughout the core (Figs. 7, 8 and 9) with samples ranging from over 2/3 orange glass (74002,97) to approximately 80% black devitrified glass (74001,374-,383). Orange glass shows relatively little difference between grain sizes, making up approximately the same proportions of the coarsest through the finest sizes of all samples. In contrast, soil clasts are common in the largest sizes (Fig. 7) but become progressively rarer in finer fractions (Figs. 8, 9). Crystallized grains (mostly as part of glass droplets) increase in finer sizes, at the expense of black devitrified glass. Trends as well as inflection points which are seen in the coarsest sizes (Fig. 7) are generally also seen in the finer sizes (Figs. 8, 9), so discussion of trends in one figure is generally applicable to all. Orange glass is very rare from the base of the core to 10 cm in 74001, is rare between 10 cm in 74001 and 25 cm in 74002, and becomes increasingly abundant between 25 cm and 12 cm in 74002. It averages 60% of the fines at the top of 74002. Pyroxene generally occupies the same proportion of all samples, but olivine is most abundant below 15 cm of 74001, above which it undergoes a sharp decrease. Black, devitrified glass makes up a relatively constant proportion of the cores from the base of 74001 to 25 cm of 74002, and it declines rapidly from 25 to 13 cm of 74002. Devitrified glass plus mineral grains make up a relatively constant 30 - 40% of the top of 74002.

C. Particle Morphology

Morphology (external shape and degree of fracture) of black particles (Fig. 10) varies differently from that of orange (Fig. 11) particles, and does not vary as much, and seems to show more correspondence to stratification than variation in the morphology of the orange particles. Maxima in spheres and single droplets occur at 20 cm in 74002 (-,93) and 15-17 cm in 74001 (-,378 and -,379). Compound particles, in contrast, are at a maximum in the massive unit in 74001 (7-13 cm). Orange particles are more abundant in 74002 and show stratal-related morphological changes in this core more prominently than do the black particles.

Fractured and compound orange particles are at a minimum in the massive strata between 10 and 15 cm of 74002, and show a major increase at 15 cm to the base of the core. Fragmented orange particles are most abundant in mid-74001, and entire unbroken orange droplets are of greatest abundance between 10 and 15 cm of 74002.

In nearly all samples, there were a few orange glass particles with a variety of shapes including teardrop, fractured teardrop and rod or cylinder. Because of the low number of such particles, it was not possible to analyze for trends.

SIZE SUMMARY, 74002 AND 74001 GRAIN MOUNTS

	.5 - 1 mm 1		.25 - .5 mm 2		.12 - .25 mm 3		.06 - .12 mm 4		.01 - .06 mm		under .01 mm		
Sample No.	No. of Points	% of Points	No. of Points	% of Points	No. of Points	% of Points	No. of Points	% of Points	No. of Points	% of Points	No. of Points	% of Points	Points
					DRIVE	TUBE	74002						
-,99	0	0	4	0.8%	8	1.6%	43	8.6%	138	27.6%	307	61.4%	500
-,98	0	0	2	0.4%	18	3.6%	53	10.6%	140	28.0%	288	57.6%	500
-,97	0	0	9	1.8%	23	4.6%	53	10.6%	136	27.2%	279	55.8%	500
-,96	1	0.2%	7	1.4%	25	5.0%	51	10.2%	150	30.0%	269	53.8%	500
-,95	0	0	4	0.8%	17	3.4%	51	10.2%	162	32.4%	266	53.2%	500
-,94	0	0	6	1.2%	35	7.0%	69	13.8%	140	28.0%	250	50.0%	500
-,93	0	0	4	0.8%	7	1.4%	36	7.2%	166	33.2%	287	57.4%	500
-,92	0	0	2	0.4%	18	3.6%	60	12.0%	174	34.8%	246	49.2%	500
-,91	This slide appeared anomalously thin and fine-grained, and was probably improperly prepared												
-,90	0	0	3	0.6%	11	2.2%	42	8.4%	179	35.8%	266	53.2%	500
					DRIVE	TUBE	74001						
-,374	0	0	2	0.6%	10	2.8%	40	11.3%	88	24.9%	214	60.4%	354
-,375	0	0	0	0	19	4.4%	27	6.2%	115	26.5%	273	62 9%	434
-,376	0	0	0	0	7	2.5%	14	5.0%	65	23.1%	195	69.3%	281
-,377	0	0	3	0.6%	7	1.5%	20	4.4%	102	22.3%	315	68.9%	457
-,378	0	0	0	0	6	1.9%	15	4.8%	80	25.9%	208	67.3%	309
-,379	0	0	1	0.2%	7	1.6%	19	4.2%	101	22.4%	322	71.5%	450
-,380	0	0	1	0.4%	4	1.5%	15	5.7%	62	23.7%	180	68.7%	262
-,381	0	0	2	0.4%	7	1.4%	32	6.2%	134	25.9%	342	66.2%	517
-,382	0	0	2	0.8%	4	1.5%	14	5.4%	66	25.5%	173	66.8%	259
-,383	0	0	5	0.9%	5	0.9%	28	5.3%	156	29.2%	339	63.6%	533

Table. V. Grain size data, 74002/74001 grain mounts.

Table VI. COMPOSITIONAL SUMMARY FOR COARSER SIZE CLASSES, GRAIN MOUNTS FROM DRIVE TUBE 74002

		Orange Glass		Black "Glass"		Pyroxene		Olivine		Soil Clasts		
Sample No.	Size Class	No. of Points	% of Total	No. of Points	% of Total	No. of Points	% of Total	No. of Points	% of Total	No. of Points	% of Total	Total Points Counted
-,99	0.12-.25mm	121	56%	65	30%	4	2%	2	1%	22	11%	214
	0.06-.12mm	128	45%	87	31%	'43	11%	18	6%	19	7%	284
	0.01-.06mm	148	61%	45	19%	28	12%	15	6%	6	2%	242
-,98	0.12-.25mm	114	53%	76	35%	5	2%	6	3%	15	7%	216
	0.06-.12mm	109	47%	56	24%	47	20%	15	6%	6	3%	233
	0.01-.06mm	164	59%	49	18%	44	16%	16	6%	4	1%	276
-,97	0.12-.25mm	141	70%	53	26%	6	3%	0	0%	0	0%	200
	0.06-.12mm	159	67%	48	20%	17	7%	13	6%	0	0%	236
	0.01-.06mm	200	73%	32	12%	30	11%	11	4%	0	0%	272
-,96	0.12-.25mm	112	53%	91	43%	4	2%	3	1%	0	0%	210
	0.06-.12mm	114	35%	122	38%	67	21%	20	6%	0	0%	322
	0.01-.06mm	171	42%	120	29%	78	19%	38	9%	0	0%	407
-,95	0.12-.25mm	97	43%	112	50%	15	6%	1	1%	0	0%	226
	0.06-.12mm	105	37%	94	33%	64	23%	19	7%	0	0%	282
	0.01-.06mm	143	44%	83	26%	65	20%	31	9%	0	0%	322
-,94	0.12-.25mm	92	44%	101	48%	10	5%	5	2%	0	0%	208
	0.06-.12mm	96	28%	154	44%	62	18%	35	10%	0	0%	347
	0.01-.06mm	170	35%	142	30%	112	23%	58	12%	0	0%	481
-,93	0.12-.25mm	68	32%	121	57%	19	9%	3	1%	0	0%	211
	0.06-.12mm	95	24%	175	44%	83	21%	48	12%	0	0%	401
	0.01-.06mm	104	26%	151	38%	99	25%	47	12%	0	0%	401
-,92	0.12-.25mm	49	25%	139	70%	10	5%	2	1%	0	0%	200
	0.06-.12mm	50	16%	187	61%	47	15%	21	7%	0	0%	305
	0.01-.06mm	55	18%	146	48%	73	24%	30	10%	0	0%	304
-,91	0.12-.25mm	51	15%	210	60%	57	16%	32	9%	0	0%	350
	0.06-.12mm	56	16%	199	56%	63	18%	35	10%	0	0%	353
	0.01-.06mm	81	24%	158	47%	71	21%	29	9%	0	0%	339
-,90	0.12-.25mm	36	8%	325	73%	52	11%	31	7%	0	0%	444
	0.06-.12mm	67	17%	237	59%	33	16%	18	8%	0	0%	211
	0.01-.06mm	46	17%	174	66%	36	14%	17	6%	0	0%	263
		COMPOSITIONAL SUMMARY FOR COARSER SIZE CLASSES, GRAIN MOUNTS FROM DRIVE TUBE 74001										
-,374	0.12-.25mm	49	17%	225	80%	19	6%	8	3%	0	0%	300
	0.06-.12mm	56	18%	188	62%	37	12%	22	7%	0	0%	304
	0.01-.06mm	28	14%	123	60%	36	18%	17	8%	0	0%	204
-,375	0.12-.25mm	36	18%	136	70%	16	8%	7	4%	0	0%	195
	0.06-.12mm	147	18%	533	63%	95	12%	48	6%	0	0%	823
	0.01-.06mm	76	18%	213	49%	94	22%	48	11%	0	0%	433
-,376	0.12-.25mm	19	9%	146	73%	26	13%	10	5%	0	0%	201
	0.06-.12mm	33	17%	124	61%	25	12%	14	7%	0	0%	200
	0.01-.06mm	45	18%	114	46%	57	23%	28	11%	0	0%	249
-,377	0.12-.25mm	4	4%	92	81%	13	11%	5	4%	0	0%	114
	0.06-.12mm	13	6%	159	72%	39	17%	11	5%	0	0%	222
	0.01-.06mm	19	9%	105	50%	62	29%	24	11%	0	0%	212
-,378	0.12-.25mm	3	2%	116	78%	15	10%	15	10%	0	0%	149
	0.06-.12mm	24	9%	156	56%	56	20%	40	14%	0	0%	278
	0.01-.06mm	22	9%	113	45%	74	30%	41	16%	0	0%	250
-,379	0.12-.25mm	14	7%	154	77%	19	10%	13	7%	0	0%	200
	0.06-.12mm	27	9%	190	63%	42	14%	41	14%	0	0%	300
	0.01-.06mm	28	14%	95	47%	39	19%	36	18%	0	0%	200
-,380	0.12-.25mm	7	4%	146	73%	23	12%	23	12%	0	0%	200
	0.06-.12mm	15	6%	156	66%	37	16%	38	16%	0	0%	246
	0.01-.06mm	26	13%	92	46%	39	20%	43	21%	0	0%	200
-,381	0.12-.25mm	28	6%	333	74%	47	10%	52	12%	0	0%	450
	0.06-.12mm	30	7%	251	61%	64	15%	69	17%	0	0%	414
	0.01-.06mm	36	12%	123	40%	74	24%	84	27%	0	0%	308
-,382	0.12-.25mm	34	8%	262	68%	44	11%	47	12%	0	0%	388
	0.06-.12mm	14	7%	122	58%	36	17%	37	17%	0	0%	209
	0.01-.06mm	32	15%	82	38%	44	21%	57	27%	0	0%	214
-,383	0.12-.25mm	13	6%	143	72%	20	10%	24	12%	0	0%	200
	0.06-.12mm	15	7%	143	62%	37	16%	32	14%	0	0%	228
	0.01-.06mm	18	9%	95	42%	47	24%	38	19%	0	0%	200

Table VII. MORPHOLOGICAL VARIATIONS IN ORANGE AND BLACK PARTICLES, GRAIN MOUNTS FROM DRIVE TUBE 74002

ORANGE PARTICLES, 3 Ø size class

	Spherical droplets				Ovoid droplets				Indet. equant		Compound		
	Complete		Broken*		Complete		Broken		Fragments		Particles		
Sample No.	No. of Points	% of Points	No. of Points	% of Points	No. of Points	% of Points	No. of Points	% of Points	No. of Points	% of Points	No. of Points	% of Points	Total Points Counted
-,99	23	4.9%	124	22.0%	8	1.7%	122	26.2%	164	35.3%	23	4.9%	465
-,98	33	5.9%	131	23.2%	23	4.1%	136	24.1%	203	36.0%	38	6.7%	564
-,97	96	18.3%	96	18.3%	47	9.0%	127	24.2%	118	22.5%	40	7.6%	524
-,96	35	11.0%	79	25.0%	32	10.1%	92	29.1%	58	18.4%	19	6.0%	316
-,95	45	16.4%	63	23.0%	15	5.5%	56	20.4%	61	22.3%	34	12.4%	274
-,94	16	3.2%	117	23.8%	14	2.8%	127	25.8%	185	37.0%	58	11.9%	492
-,93	9	3.4%	74	24.7%	88	2.9%	69	24.9%	81	29.2%	34	12.3%	277
-,92	7	2.9%	58	24.4%	4	1.7%	62	26.0%	85	33.7%	33	14.8%	248
-,91	12	7.7%	37	23.9%	4	2.6%	44	28.4%	46	29.7%	Indet. poor slide		155
-,90	15	10.3%	25	17.2%	5	3.4%	27	18.6%	48	33.1%	25	17.2%	145

BLACK PARTICLES, 3 Ø size class

	Spheres*		Ovoid Droplets		Broken equant fragments		Compound Particles				Total points Counted
							Spheres		Ovoid particles		
-,99	9	5%	4	2%	41	20%	68	34%	78	39%	200
-,98	6	6%	4	4%	16	16%	28	28%	48	47%	102
-,97	9	5%	6	3%	44	21%	54	25%	92	45%	205
-,96	11	5%	12	5%	46	22%	58	26%	87	42%	214
-,95	14	7%	10	5%	43	21%	59	28%	76	37%	202
-,94	17	7%	13	6%	35	15%	74	31%	103	43%	236
-,93	23	11%	15	7%	28	14%	55	27%	85	41%	206
-,92	18	9%	10	5%	40	20%	58	28%	76	37%	202
-,91	17	7%	9	4%	47	19%	78	31%	102	40%	253
-,90	14	7%	4	2%	38	19%	61	30%	83	41%	200

***Note that orange and black particles show similar, but not identical forms.**

MORPHOLOGICAL VARIATIONS IN ORANGE AND BLACK PARTICLES, GRAIN MOUNTS FROM DRIVE TUBE 74001

ORANGE PARTICLES, 3 Ø size class

	Spherical Droplets				Ovoid Droplets				Indet. equant		Compound		
	Complete		Broken*		Complete		Broken		Fragments		Particles		
Sample No.	No. of Points	% of Points	No. of Points	% of Points	No. of Points	% of Points	No. of Points	% of Points	No. of Points	% of Points	No. of Points	% of Points	Total Points Counted
-,374	13	6%	31	15%	7	4%	28	14%	86	43%	37	18%	202
-,375	7	3%	25	12%	6	3%	34	16%	101	49%	32	16%	205
-,376	12	6%	24	12%	11	5%	44	21%	74	36%	43	21%	208
-,377	4	3%	13	9%	7	5%	28	19%	58	40%	32	22%	144
-,378	12	7%	18	11%	6	4%	32	20%	64	40%	28	18%	160
-,379	9	4%	18	9%	13	6%	36	18%	88	44%	37	18%	201
-,380	11	5%	28	14%	9	4%	24	12%	84	41%	48	24%	204
-,381	11	5%	20	10%	10	5%	43	21%	76	37%	44	22%	204
-,382	11	6%	26	15%	10	5%	41	19%	83	38%	47	21%	219
-,383	9	4%	25	10%	10	4%	51	21%	84	34%	69	28%	248

BLACK PARTICLES, 3 Ø size class

	Spheres*		Ovoid Droplets		Broken equant fragments		Compound Particles				Total points Counted
							Spheres		Ovoid particles		
-,374	26	7%	26	7%	13	20%	92	25%	150	51%	367
-,375	24	5%	39	8%	87	18%	135	28%	198	41%	483
-,376	14	4%	10	3%	48	14%	86	25%	158	46%	344
-,377	18	5%	11	3%	55	15%	66	18%	215	59%	365
-,378	54	10%	16	3%	70	13%	107	20%	289	54%	536
-,379	34	12%	11	4%	31	11%	56	20%	148	53%	280
-,380	37	7%	36	7%	68	13%	88	17%	291	56%	520
-,381	26	6%	39	9%	48	11%	61	14%	262	60%	437
-,382	24	6%	24	6%	36	9%	64	16%	252	63%	400
-,383	31	7%	13	3%	49	11%	66	15%	282	64%	441

***Note that orange and black particles show similar, but not identical forms.**

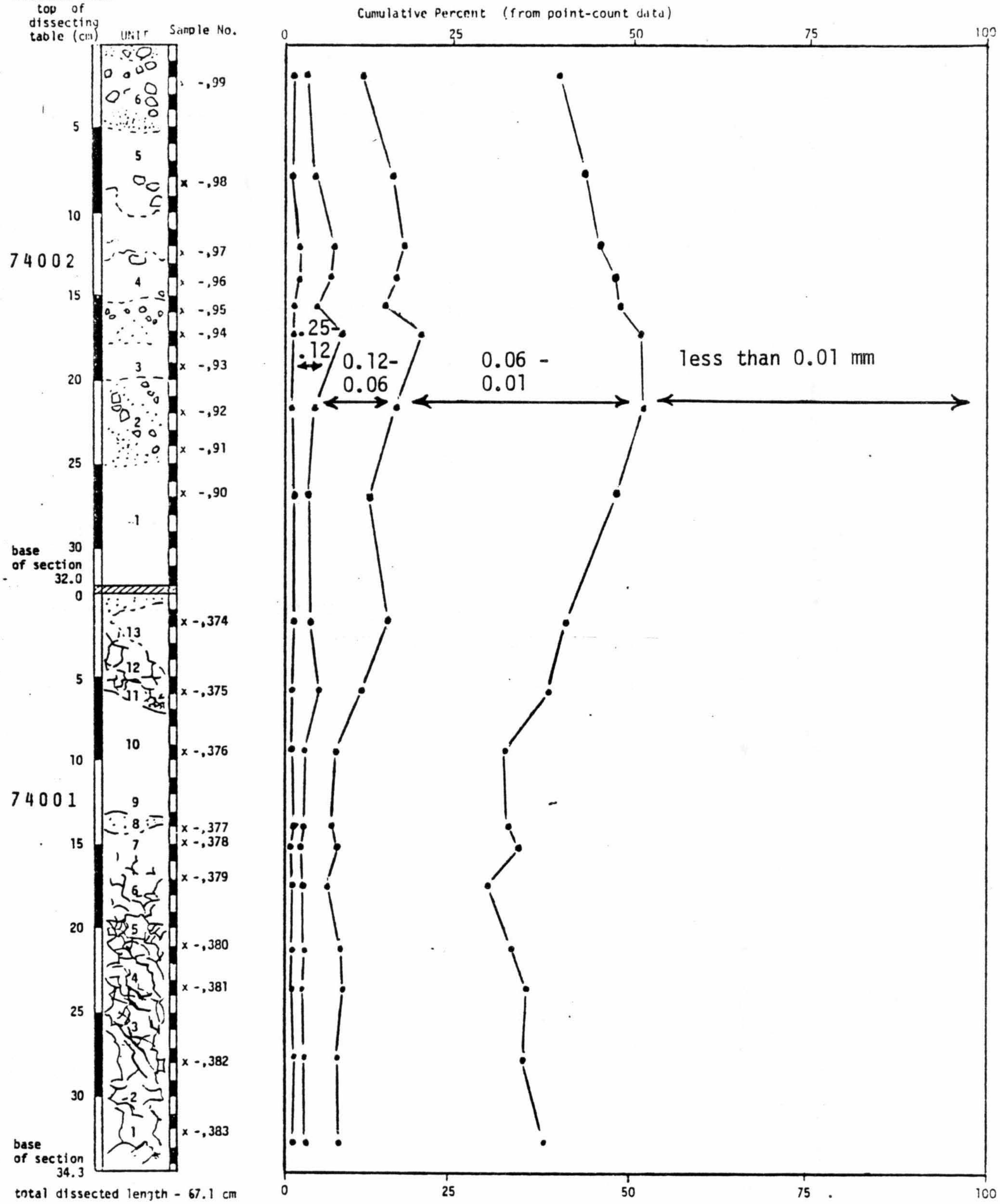

Fig. 6 . Grain size versus depth in drive tubes 74002/74001.

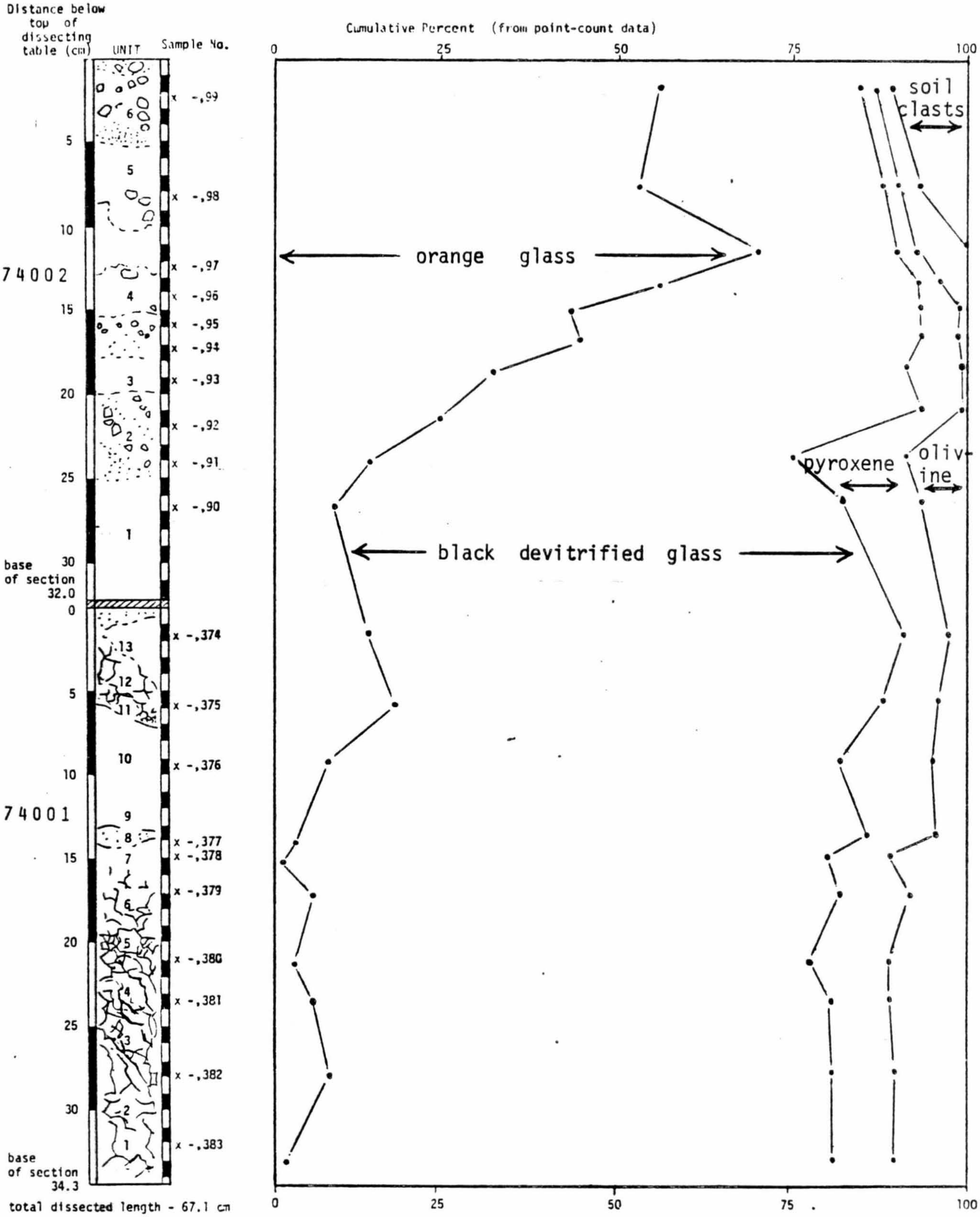

Fig. 7 . Compositional proportions of 0.12 - 0.25mm particles, drive tubes 74002/1.

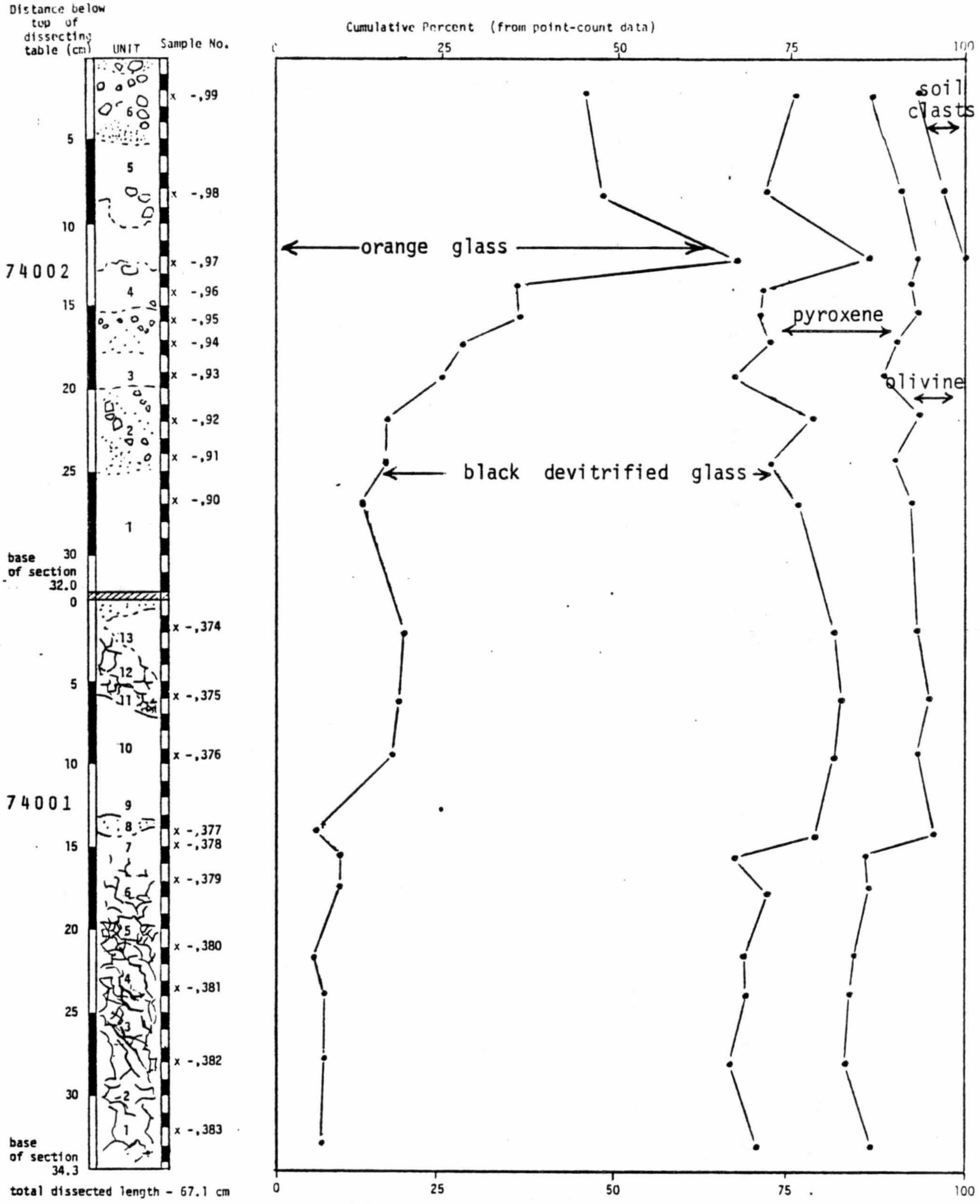

Fig. 8 . Compositional proportions of 0.06 - 0.12 mm particles, drive tubes 74002/1.

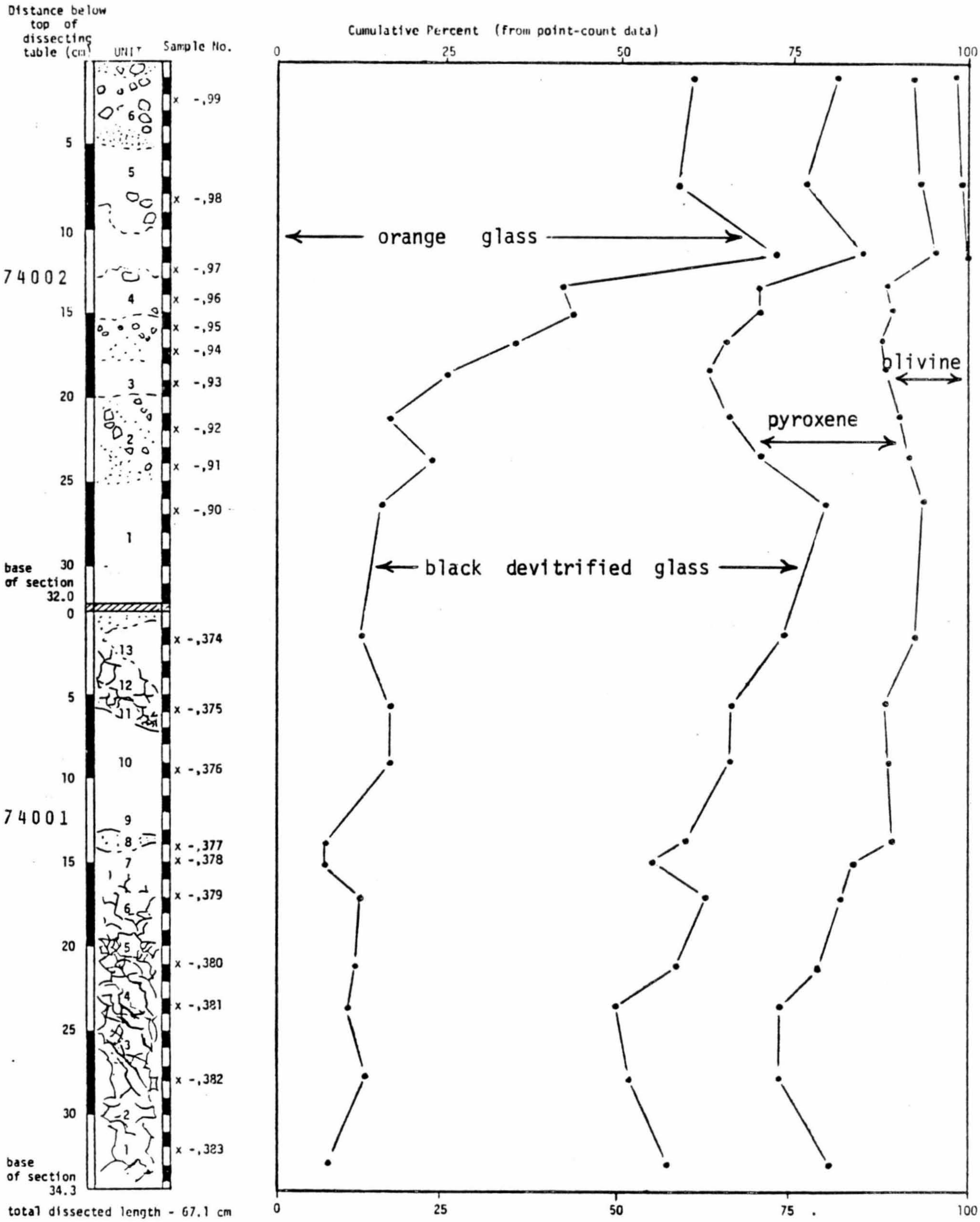

Fig. 9 . Compositional proportions of 0.01 - 0.06 mm particles, drive tubes 74002/1.

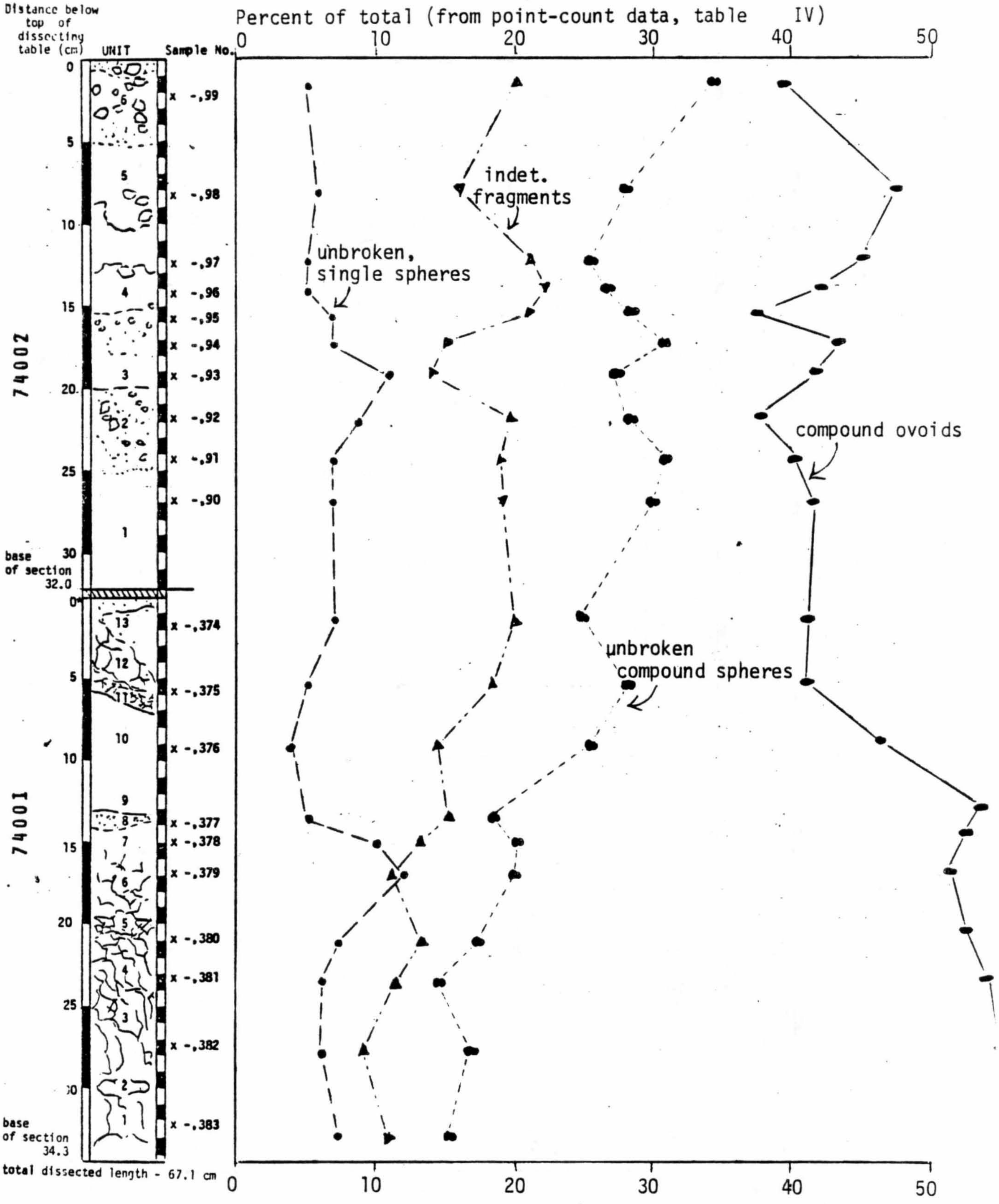

Fig. 10. Changes in particle morphology of black particles from drive tubes 74002/74001. Cumulative percent is not used here in order to better illustrate types of co-variation and trends in particle abundance.

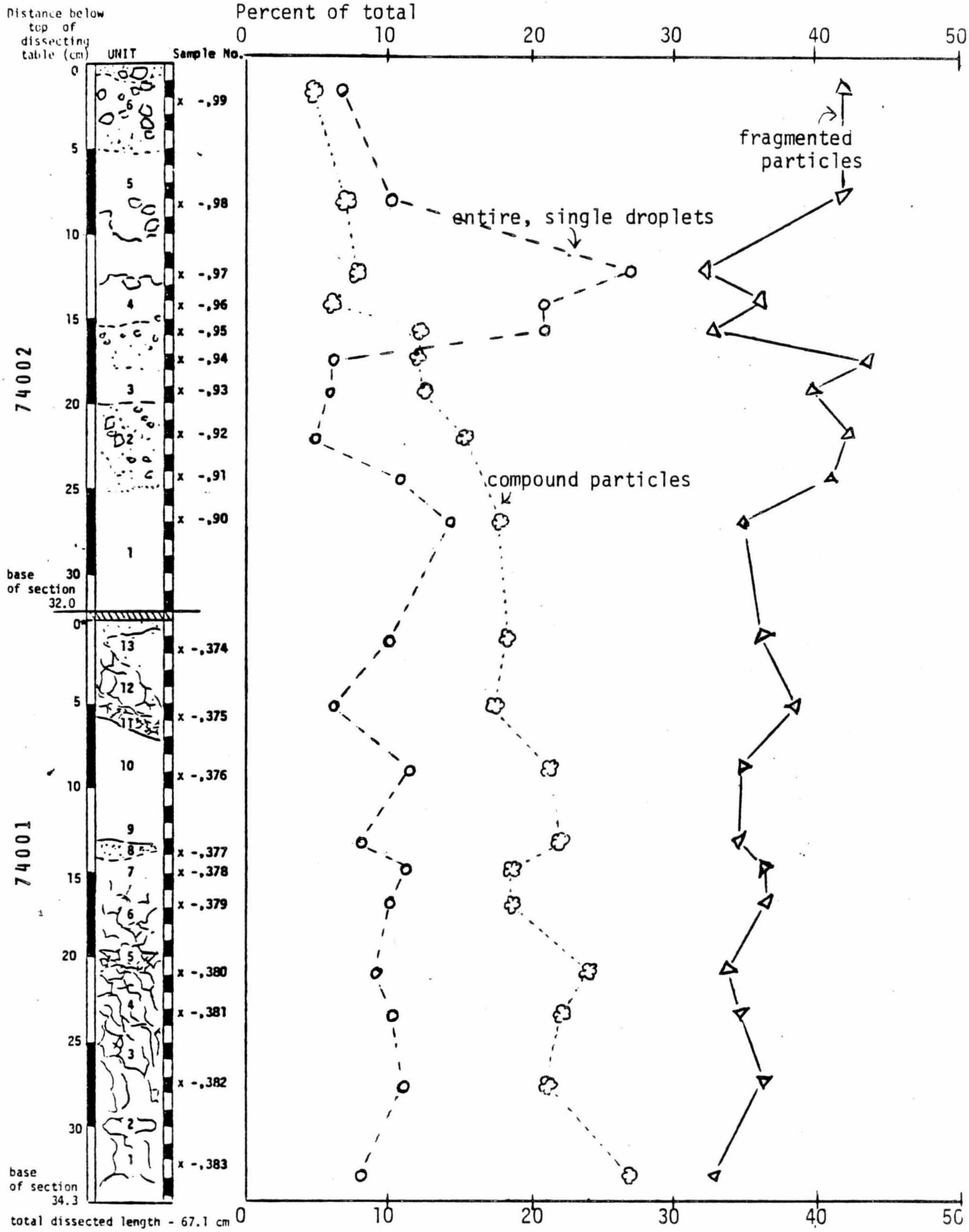

Fig. 11. Changes in morphology of orange particles from 74002/74001. Cumulative percentages are not used here in order to better illustrate co-variation in trends.

6. Stratigraphic units

A. Fine-Grained Parts of 74001 and 74002

Although three major units and nine radiographic units were recognized in 74001 and 10 in 74002, on the basis of grain mount and dissection petrography, 13 units were identified in 74001 and 7 in 74002 (Figs. 12 and 13). The lowest five in 74001 are similar compositionally but were distinguished on the basis of grain morphology and depositional structure. The next five are similar in physical properties but show notable difference in composition and texture. Like the lowest five units the upper three units in 74001 are similar compositionally but were distinguished on the basis of structures that resemble those of the lower units. In 74002 each of the 6 units differs from the others both in texture and in composition; the small-scale structures seen in 74001 are absent from 74002.

The lowest five units in 74001, from 34.3 cm (bottom of the core) up to 19.0 cm, form the lower major unit. Under the binocular microscope these are seen to be flaky cohesive to friable, dull in appearance, and in grain mount, are very low in orange glass, high in black devitrified glass as well as mineral grains, with approximately equal amounts of pyroxene and olivine. Individual units are differentiated on internal droplet succession. At the top of each of the five units, multiple droplets are most abundant, and single droplets prevail at the base of each unit. The change from single to multiple droplets at unit boundaries is relatively abrupt, but changes within units are gradual. Specifics of unit boundaries and samples included in each unit are presented in Figs, 12, 13.

The middle five units in 74001 are relatively massive and cohesive, with abundant coarse vitreous particles and are considered the middle major unit. Unit 6, from 19.0 up to 15.5 cm, is relatively massive and cohesive and shows no internal transition from one droplet to another, but is compositionally similar to units 1-5. Unit 7, from 15.5 cm up to 14.5 cm is very cohesive, coarse-grained, and is similar to units 1-5 compositionally, in being low in orange glass and high in olivine. Unit 8, another thin unit, is found between 14.5 and 13.5 cm and is friable, relatively fine grained, and contains little olivine, and orange glass. Orange glass exhibits a major increase by unit 9 and 10. Both units are very cohesive with units from 13 to 10.0 cm being noticeably coarser, with a concentration of large droplets but from 10.0 to 7.0 cm being slightly finer. Units 11, 12 and 13 are similar to the lower part of the area, and comprise the upper major unit. These are friable and relatively fine-grained, and show the multiple double to single droplet succession described for the basal five units. However, orange glass at the top of this lower core is much more abundant (18% vs 7%) and olivine is as rare as it is in the cohesive coarse units in the middle of the core.

Fig. 12. PRELIMINARY STRATIGRAPHIC SUMMARY, DRIVE TUBE 74002

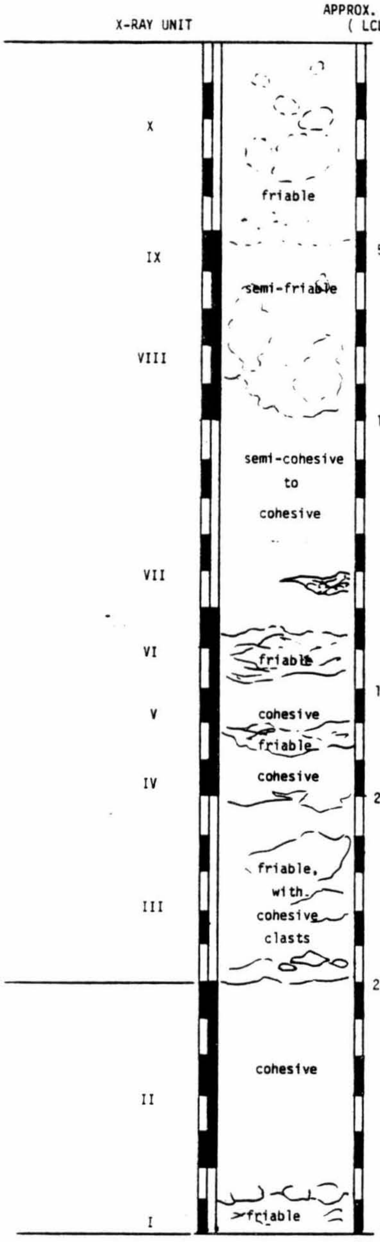

APPROX. UNIT BOUNDARIES (LCL INVENTORY)	UNIT	LITHOLOGY
	6	Dark, fine-grained soil with abundant orange clasts. Matrix averages 75% of total, and consists almost completely of fragmented particles of orange and dark glass, with very small quantities of mineral grains, ropy glass, and agglutinates. Mineral grains and agglutinates increase at the top of the section. The coarse fraction includes approximately 50% cm.-sized rounded clasts of semi-cohesive orange soil, approximately 40% similar-sized clasts of dark soil, and less than 10% of mare basalt fragments.
5.5 distinct, irregular	5	Dark, fine-grained soil with large, irregular orange clasts. Dark matrix averages 60% of total, and consists almost completely of fragmented particles of orange and dark glass; agglutinates and other similar particles are rare or not present. b Orange clasts are 2 to 3 cm. in diameter, friable, interfinger with matrix, and are oriented with long axis vertical.
10.0 distinct, interfingering	4	Orange Soil zone. Semi-cohesive stratum of very fine-grained orange droplets and droplet fragments, with 25 - 50% dark glass, as fine-grained as ornage, both randomly scattered through orange soil, and occurring as linear, subvertical inclusions. Orange is most abundant at 10 - 13 cm. but is very noticeable to 17 cm.
17.0 distinct, semi-planar	3	Moderately orange soil. Mixed friable-cohesive interval of fine-grained orange and dark soil, with dark predominating, but with orange noticeable.
20.0 distinct, nearly planar to irregular, depending on dissection and position in core	2	Dark soil, fine-grained, with predominant particles of black, devitrified glass which range from single spheres to compounded, fragmented ellipsoids. Orange glass is not as abundant as above, making up less than 20% of the total. This interval is friable, and contains cohesive clasts that appear to have the same composition as the matrix.
25.0 semi-planar in dissection, but appears transitional in X-ray, with fragments in unit 2 matching cavities on upper surface of unit 1.	1	Dark soil, as unit 2 in composition and size distribution, but very cohesive throughout, instead of being friable, with cohesive clasts. Similar lithology continues into the top of 74001, immediately below this core.
32.0 cm. base of core		

Fig. 13

PRELIMINARY STRATIGRAPHIC SUMMARY, DRIVE TUBE 74001

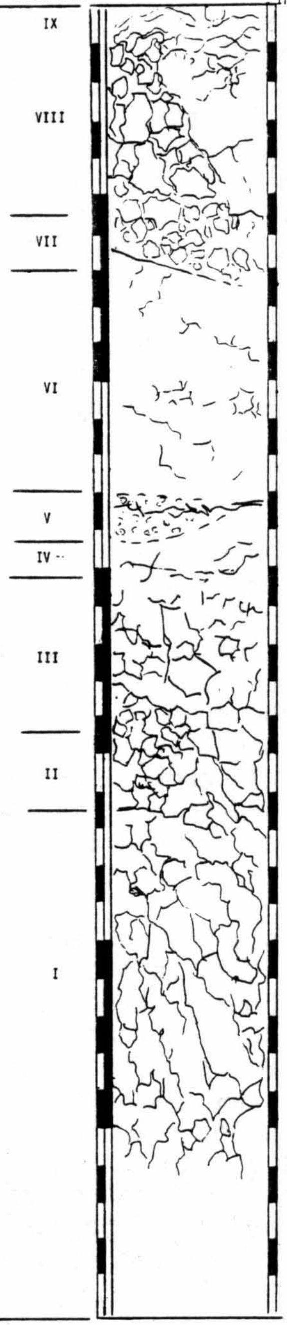

SAMPLING INTERVAL	MAJOR UNIT	LITHOLOGY	UNIT	SAMPLES	LITHOLOGIC DIFFERENCES FROM MAJOR UNIT
0.0	C	flaky cohesive, dull in appearance, poorly sorted with abundant devitrified fines, random internal fabric.	13	,21 ,26- ,30	internal droplet succession multiple double single
2.5			12	,31- ,37	internal droplet succession multiple double single
5.5			11	,38- ,41	seems transitional to B and C; has dull appearance as above, vitreous glass and compound droplets as below
7.0	B	distinct, planar contact massive and strongly cohesive, relatively reflective and sparkly in appearance, relatively coarse and sorted with abundant vitreous glass droplets, internally stratified.	10	,42- ,46	characteristics of major unit
10.0			9	,47- ,53	concentration of large droplets
13.5			8	,54 ,55	relatively fine-grained
14.5			7	,56 ,57	relatively coarse-grained
15.5			6	,58- ,64	characteristics of major unit
19.0			5	,65- ,69	internal droplet succession multiple double single
21.5	A	flaky cohesive, dull in appearance, poorly sorted with abundant devitrified fines, random internal fabric	4	,70- ,74	internal droplet succession, as above
24.0			3	,75- ,81	internal droplet succession as above
27.0			2	,82- ,88	internal droplet succession as above
30.0			1	,89- ,97	relatively homogeneous unit, with scattered but large compound droplets, unusual horizontal grain alignment at 30 cm. (top of unit).
34.3 (base of core)					

In the upper core, 74002, unit 1 (32 up to 25 cm) is fairly cohesive, with very abundant dark compound droplets, a very few orange glass droplets. Unit 2 (25 - 20 cm) is moderately friable, is also low in orange glass, with a maximum in dark droplets and a minimum in mineralized grains. Unit 3 (20 - 17 cm) shows a marked increase in orange glass, to intermediate abundances, and has numerous compound droplets. The maximum orange glass is found in unit 4 (17 - 10 cm). In this unit, there is also very little fragmentation of particles, in contrast to other units. Unit 5 (5.5 to 10 cm) is darker than unit 4, but contains a similar abundance of orange. However, particles in this unit are very fragmented, in contrast to those of the stratum immediately below. Unit 6 (5.5 cm up to the lunar surface) is characterized by the presence of agglutinates and abundant clasts of orange and dark soil. Although this unit is a grayish to dark orangish-gray, it does not have the ropy glasses found in nearby surficial gray soils (74240 and 74260).

B. Properties of Upper 5.5 cm of 74002

The top 5.5 cm of 74002 differs markedly from the rest of the core in that it contains abundant soil clasts, agglutinates, and lithified rock fragments. In X-radiograph, soil above 5.5 cm is much less compact than soil below that depth. Glass particles, as seen in grain mounts, are much more fragmented in the upper part of the core. All this evidence indicates that the upper part of the core is a gardened detrital zone that differs from the cohesive orange and black glass succession below. Between 10 and 5.5 cm soil is relatively compact and contains no agglutinates or detrital rock fragments. Because of this inconsistent evidence, it is not clear whether the section between 5.5 and 10 cm is gardened, Shorty fall-back, or something else.

Above 5.5 cm, the core is packed with clasts of orange and dark soil, and may be regarded as very coarse-grained, with as much as 49.5% > 1 mm (Table IX). Because of the friability of the soil clasts, there is a decrease in clast size toward the top of the core, but mm-sized clasts of orange soil occur at the very top of the core, as seen in upper surface photos 5-77-27498 and 27499. Fragmentation, as best seen in orange particles in grain mounts, is much higher in the reworked part of the section; for instance, nearly 5% of spheres and 2% of ovoid droplets are unbroken at 2.5 cm, whereas 11-18% spheres and 10% ovoid droplets are not broken in samples below 12 cm. Furthermore, in the deeper samples there are only 20% indeterminate broken particles but at 2.5 cm, there are 35%.

Composition is considered in terms of abundance of cohesive clasts > 1 mm. Such clasts are retained on the 1 mm sieve, size-sorted, classified, and weighed individually. Abundance in each size fraction is then determined by weight percentage calculations. Orange clasts make up all fragments over 10 mm, and both orange and dark clasts are ubiquitous throughout the upper part of the section. The lowest agglutinate and mare basalt fragments appear at 4.5 cm, and progressively increase to the top, (although the only "large" cohesive particles at the very surface are agglutinates).

Table VIII.
TEXTURAL PROPERTIES OF THE UPPER 5.5 CM OF DRIVE TUBE 74002

Depth (mm)	Sample Nos.	Over 10 mm		4 - 10 mm		2 - 4 mm		1 - 2 mm		Under 1 mm		Total Wt.
		Wt.	%	Wt.	%	Wt.	%	Wt.	%	Wt.	%	
0 - 1	-,2 -,3	.....	.....	.....	.....	.....	.....	0.011 gm	0.6%	1.934 gm	99.4%	1.945 gm
1 - 2	-,4 -,5	.....	.....	.....	.....	.....	.....	0.045 gm	2.0%	2.108 gm	98.0%	2.233 gm
2 - 3	-,6 -,7	.....	.....	.....	.....	.....	.....	0.053 gm	2.1%	2.445 gm	97.9%	2.498 gm
3 - 4	-,8 -,9	.....	.....	.....	.....	0.213 gm	7.9%	0.060 gm	2.2%	2.426 gm	89.9%	2.699 gm
4 - 5	-,10-,11	.....	.....	.....	.....	0.229 gm	9.3%	0.075 gm	3.0%	2.150 gm	87.6%	2.454 gm
5 -15	-,87-,89 -,2068-71	.....	.....	1.354 gm	15.2%	0.391 gm	4.4%	0.270 gm	3.0%	6.877 gm	77.3%	8.892 gm
15 -25	-,84-,86 -,2064-67	2.911 gm	22.6%	1.370 gm	10.6%	0.176 gm	1.4%	0.239 gm	1.8%	8.224 gm	63.6%	12.920 gm
25 -35	-,80-,83 -,2061-63	5.334 gm	35.2%	1.456 gm	9.6%	0.309 gm	2.0%	0.392 gm	2.6%	7.647 gm	50.5%	15.138 gm
35 -45	-,77-,79 -,2058-60	2.178 gm	16.6%	1.414 gm	10.7%	0.269 gm	2.0%	0.365 gm	2.8%	8.932 gm	67.9%	13.158 gm
45 -55	-,74-,76 -,2055-25	.....	.....	0.985 gm	7.0%	0.253 gm	1.8%	0.173 gm	1.2%	12.599 gm	89.9%	14.010 gm

Table IX.
COMPOSITION OF UPPER (DETRITAL) PART OF 74002

size class		4 - 10 mm							2 - 4 mm							1 - 2 mm								
		orange clasts		dark soil clasts		basalt fgms.			orange clasts		dark soil clasts		basalt fgms.			orange clasts		dark soil clasts		basalt clasts		agglutin-ates		
interval	sample nos.	Wt.	%	Wt.	%	Wt.	%	sum	Wt.	%	Wt	%	Wt.	%	sum	Wt.	%	Wt.	%	Wt.	%	Wt.	%	sum
0 - 1 mm	,2 ,3	....	...	....	...	....	...	.....	....	...	....	...	....	...	.....	....	...	....	...	....	...	.011	100%	0.011
1 - 2 mm	,4 ,5	....	...	....	...	....	...	.....	....	...	....	...	....	...	.....	.025	56%	....	...	....	...	.020	44%	0.045
2 - 3 mm	,6 ,7	....	...	....	...	....	...	.....	....	...	....	...	....	...	.....	.037	69%	....	...	....	...	.016	31%	0.053
3 - 4 mm	,8 ,9	....	...	....	...	....	...	.....	.107	50%	.071	33%	.035	17%	0.213	.051	85%	....	...	.003	5%	.006	10%	0.060
4 - 5 mm	,10,11	....	...	....	...	....	...	.....	.191	83%	....	...	.038	17%	0.229	.066	88%	....	...	....	...	.009	12%	0.075
5 -15 mm	,87-,89 and,2068-71	.839	62%	.061	5%	.444	33%	1.344	.245	57%	.138	32%	.050	11%	0.433	.130	48%	.093	34%	.020	7%	.027	10%	0.270
15 -25 mm	,84-,86 and,2064-67	.985	72%	.483	28%	....	...	1.370	.045	39%	.071	61%	....	...	0.116	.093	39%	.117	49%	.006	2%	.023	10%	0.239
25 -35 mm	,80-,83 and,2061-63	1.456	100%	...	...	....	...	1.456	.257	83%	.052	17%	....	...	0.309	.243	61%	.132	33%	.010	2%	.012	3%	0.397
35 -45 mm	,77-,79 and,2058-60	.894	63%	.520	37%	....	...	1.414	.190	65%	.101	35%	....	...	0.291	.118	33%	.238	65%	.005	1%	.004	1%	0.365
45 -55 mm	,74-,76 and,2055-57	.366	61%	.235	39%	....	...	0.601	.064	25%	.189	75%	....	...	0.253	.018	11%	.155	89%	....	...	....	....	0.173

Fig. 14.

PETROGRAPHIC VARIATIONS, UPPER 5.5 CM. OF DRIVE TUBE 74002

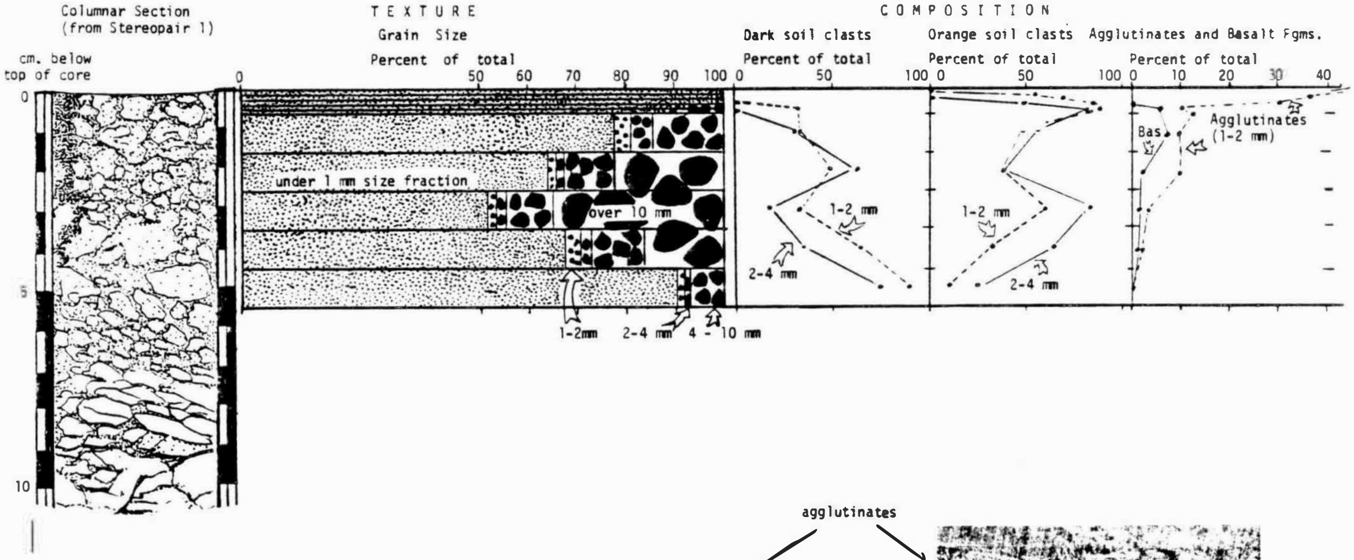

agglutinate

74002,3 (S-77-27640)
0 - 1 mm

agglutinates

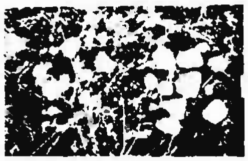

74002,5 (S-77-27641)
1 - 2 mm

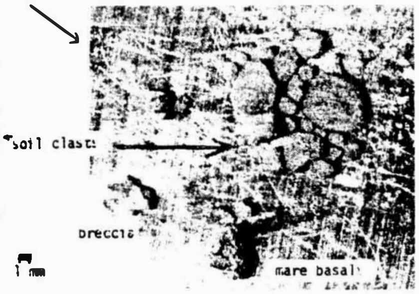

Fig. 15 A. Representative Coarse Fractions, Uppermost 5mm, 74002.

74002,9 (S-77-27643)
3 - 4 mm

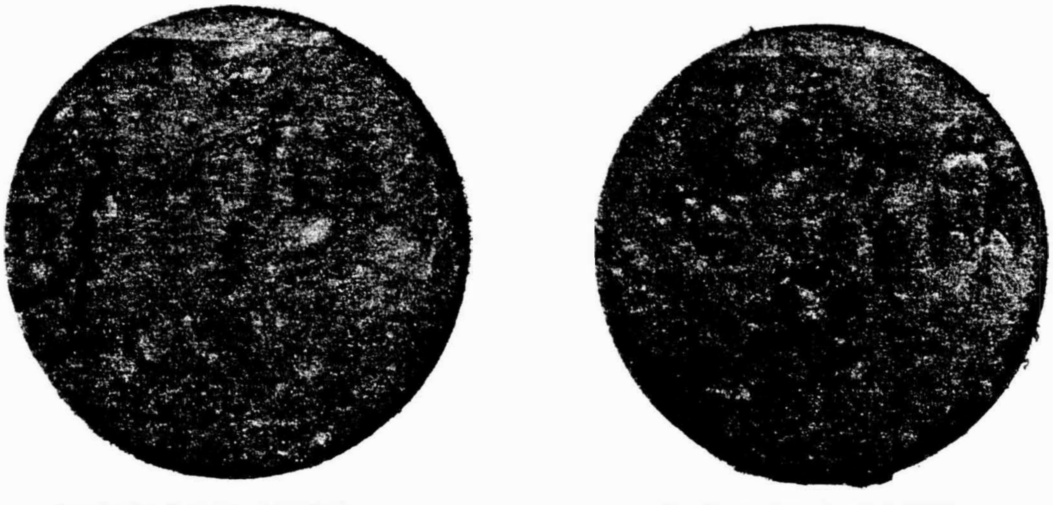

after 1st 1mm dissection (S-77-27502)

after 4th 1mm dissection (S-77-27505)

Fig. 15. B. Light clasts on transverse section across the core during 5mm dissection. Diameter in both cases is 4 cm.

C. Uppermost 5 mm

The uppermost 5 mm was dissected in 1 mm increments, from the top (Lunar surface) down to a depth of 5 mm. Three microstrata were identified in this interval; quantitative characteristics are presented in Table 1. The uppermost stratum occupies the interval between the lunar surface and 1 mm, and consists of very fine-grained drab-gray soil with 99.4% < 1 mm. The one coarse particle is an agglutinate. The next 2 mm are mixed gray and orange soil, and are somewhat coarser, containing 2% coarse material, mostly agglutinates, with a few relatively cohesive clasts of orange soil. Although the bulk of the sample is drab-gray, small orange clasts are scattered irregularly in linear and irregular clumps around the core. The clasts appear to be 1-5 mm in diameter, and occupy 5-10% of the surface of the second through fifth intervals of the 5 mm dissection. From 3 to 5 mm is a noticeable change in texture and composition. Coarse material makes up more than 10% of the sample, and there is an abundance of clasts over 5 mm in diameter. Compositionally, there is a decrease in drab-gray fines, in favor of orange soil; and fragments of mare basalt make their appearance, composing approximately 10% of the coarse fraction. Selected coarse fractions are depicted in Fig. 15a and distribution of clasts on dissection surfaces is depicted on Fig. 15b.

Table X . Textural properties of 0-5 mm of 74002

Depth	Sample	<1 mm		1-2 mm		over 2 mm		total
(mm)	No.	Wt.	%	Wt.	%	Wt.	%	(wt)
0								
	2 - 3	1.934 gm	99.4%	0.011 gm	0.6%	-----	-----	1.945 gm
1								
	4 - 5	2.188 gm	98.0%	0.045 gm	2.0%	-----	-----	2.233 gm
2								
	6 - 7	2.445 gm	97.9%	0.053 gm	2.1%	-----	-----	2.498 gm
3								
	8 - 9	2.426 gm	89.9%	0.060 gm	2.2%	0.213 gm	7.9%	2.699 gm
4								
	10 - 11	2.150 gm	87.6%	0.075 gm	3.0%	0.229 gm	9.3%	2.454 gm
5								

WORKS CITED IN TEXT

AFGIT (Apollo Field Geology Investigation Team): 1975, Documentation and environments of the Apollo 17 samples. *Astrogeology* 73 U. S. Geol. Surv. Interagency Rept. 316 p.

Bailey, N. G., and Ulrich, G. E.: 1975, Apollo 17 voice transcript pertaining to the geology of the landing site. U. S. Geol. Surv. GD-74-031, 361 p.

Butler, Jr., Patrick, *et al*.: 1973, Apollo 17 lunar sample information catalog. NASA MSC Special Publ. 03211, 447 p.

Heiken, G. H. and McKay, D. S.: 1974, Lunar deposits of possible pyroclastic origin. *Geochim. Cosmochim Acta 38*, 1703 - 1718.

Heiken, Grant, and McKay, David: 1977, A model for eruption behavior of a volcanic vent in eastern Mare Serenetatis. *Proc. Lunar Sci. Conf*. 8th, 3242 - 3255.

Kirsten, T., Horn, P., Heymann, D., Hubner, W., Storzer, D.: 1973, Apollo 17 crystalline rocks and soils: Rare gases, ion tracks, and ages. *Trans. Am. Geophys. Union 54*, 595-597.

Meyer, C., Jr., McKay, D. S., Anderson, D. H., and Butler, P. Jr.; 1975. The source of sublimates on Apollo 15 green and Apollo 17 orange glass samples. *Proc. Lunar Sci. Conf. 6th*, 1673 - 1699.

Muehlberger, W. R. *et al*.: 1973, Preliminary investigation of the Apollo 17 landing site. in *Apollo 17 Preliminary Science Report.* NASA SP-330, 6-1 through 6-91.

Wolfe, E. W., Lucchitta, B. K., Reed, V. S., Ulrich, G. E., and Sanchez, A. G.: 1975, Geology of the Taurus-Littrow Valley floor. *Proc. Lunar Sci. Conf*. 6th, 2463 - 2482.

APPENDIX

DOCUMENTATION OF DISSECTION SPLITS
AND
ALLOCATIONS TO PRINCIPAL INVESTIGATORS

Fig. 16 SAMPLE LOCATIONS, FIRST DISSECTION, DRIVE TUBE 74001

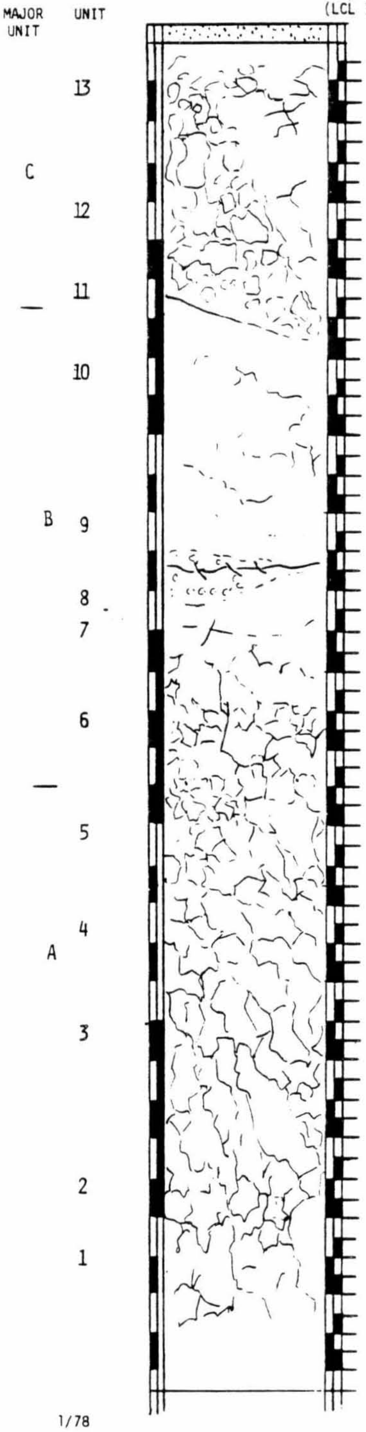

Sample Interval (LCL Inventory)	INTERVAL SAMPLES Sample No.	Vial No.	Sample Wt.	COARSE FRACTION Sample No.	Vial No.	Sample Wt.
0.0	21	9-1684	7.438	(material removed from top of core before extrusion)		
0.5	26	9-11001	0.256			
1.0	27	9-11002	1.181			
1.5	28	9-11003	1.133			
2.0	29	9-11004	1.091			
2.5	30	9-11005	1.405			
3.0	31	9-11006	1.295	32	9-11007	0.002
3.5	33	9-11008	1.445			
4.0	34	9-11009	1.347			
4.5	35	9-11010	1.561			
5.0	36	9-11011	1.286			
5.5	37	9-11012	1.504			
6.0	38	9-11013	1.454			
6.5	39	9-11014	1.354			
7.0	40	9-11015	1.373			
7.5	41	9-11016	1.411			
8.0	42	9-11017	1.468			
8.5	43	9-11018	1.307			
9.0	44	9-11019	1.499			
9.5	45	9-11020	1.507			
10.0	46	9-11021	1.513			
10.5	47	9-11022	1.329			
11.0	48	9-11023	1.445			
11.5	49	9-11024	1.569			
12.0	50	9-11025	1.368			
12.5	51	9-11026	1.331			
13.0	52	9-11027	1.656			
13.5	53	9-11028	1.158			
14.0	54	9-11029	1.356			
14.5	55	9-11030	1.384			
15.0	56	9-11031	1.525			
15.5	57	9-11032	1.440			
16.0	58	9-11033	1.495			
16.5	59	9-11034	1.521			
17.0	60	9-11035	1.603			
17.5	61	9-11036	1.298			
18.0	62	9-11037	1.531			
18.5	63	9-11038	1.431			
19.0	64	9-11039	1.447			
19.5	65	9-11040	1.577			
20.0	66	9-11041	1.450			
20.5	67	9-11042	1.394			
21.0	68	9-11043	1.514			
21.5	69	9-11044	1.427			
22.0	70	9-11045	1.590			
22.5	71	9-11046	1.333			
23.0	72	9-11047	1.641			
23.5	73	9-11048	1.394			
24.0	74	9-11049	1.505	75	9-11050	0.003
24.5	76	9-11051	1.494			
25.0	77	9-11052	1.534			
25.5	78	9-11053	1.476			
26.0	79	9-11054	1.443			
26.5	80	9-11055	1.503			
27.0	81	9-11056	1.502			
27.5	82	9-11057	1.485			
28.0	83	9-11058	1.461			
28.5	84	9-11059	1.458	85	9-11060	0.005
29.0	86	9-11061	1.556			
29.5	87	9-11062	1.488			
30.0	88	9-11063	1.555			
30.5	89	9-11064	1.410			
31.0	90	9-11065	1.656			
31.5	91	9-11066	1.490			
32.0	92	9-11067	1.486			
32.5	93	9-11068	1.580			
33.0	94	9-11069	1.534			
33.5	95	9-11070	1.306			
34.0	96	9-11071	1.165			
34.3	97	0-11072	0.894			

Fig. 17

SAMPLE LOCATIONS, SECOND DISSECTION DRIVE TUBE 74001

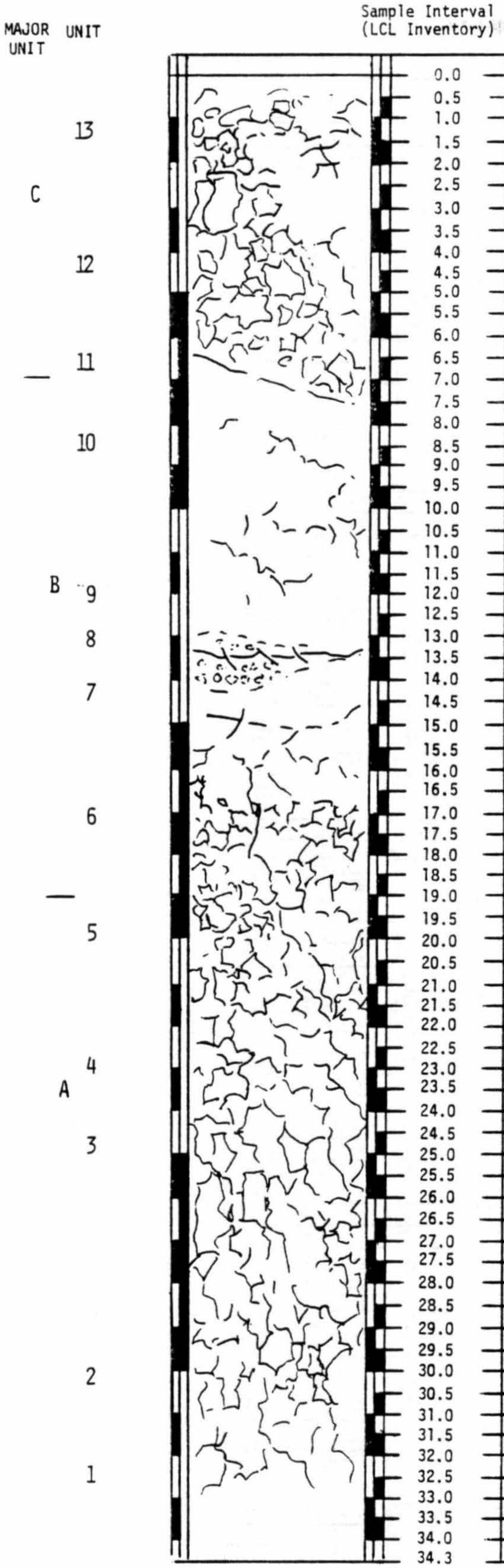

INTERVAL SAMPLES

Sample No.	Vial No.	Sample No.
removed previously		
1001	9-11101	5.560
1002	9-11102	5.087
1003	9-11103	4.447
1004	9-11104	4.249
1005	9-11105	5.089
1006	9-11106	5.265
1007	9-11107	6.314
1008	9-11108	5.400
1009	9-11109	5.734
1010	9-11110	5.782
1011	9-11111	5.200
1012	9-11112	4.806
1013	9-11113	6.690
1014	9-11114	4.967
1015	9-11115	5.287
1016	9-11116	5.632
1017	9-11117	5.990
1018	9-11118	5.451
1019	9-11119	5.821
1020	9-11120	6.876
1021	9-11121	5.774
1022	9-11122	6.332
1023	9-11123	6.132
1024	9-11124	6.178
1025	9-11125	5.166
1026	9-11126	6.080
1027	9-11127	6.162
1028	9-11128	5.695
1029	9-11129	5.832
1030	9-11130	5.781
1031	9-11131	6.077
1032	9-11132	6.402
1033	9-11133	5.223
1034	9-11134	6.049
1035	9-11135	5.894
1036	9-11136	5.765
1037	9-11137	6.416
1038	9-11138	6.060
1039	9-11139	5.562
1040	9-11140	6.448
1041	9-11141	7.052
1042	9-11142	5.666
1043	9-11143	5.606
1044	9-11144	5.736
1045	9-11145	6.538
1046	9-11146	5.403
1047	9-11147	6.713
1048	9-11148	4.871
1049	9-11149	5.341
1050	9-11150	6.548
1051	9-11151	5.808
1052	9-11152	5.678
1053	9-11153	5.728
1054	9-11154	5.688
1055	9-11155	6.331
1056	9-11156	6.342
1057	9-11157	5.996
1058	9-11158	5.053
1059	9-11159	6.294
1060	9-11160	5.758
1061	9-11161	5.668
1062	9-11162	6.622
1063	9-11163	5.864
1064	9-11164	6.684
1065	9-11165	5.434
1066	9-11166	5.737
1067	9-11167	6.157
1068	9-11168	5.506
1069	9-11169	3.385

Fig. 18

SAMPLE LOCATIONS, THIRD DISSECTION, DRIVE TUBE 74001

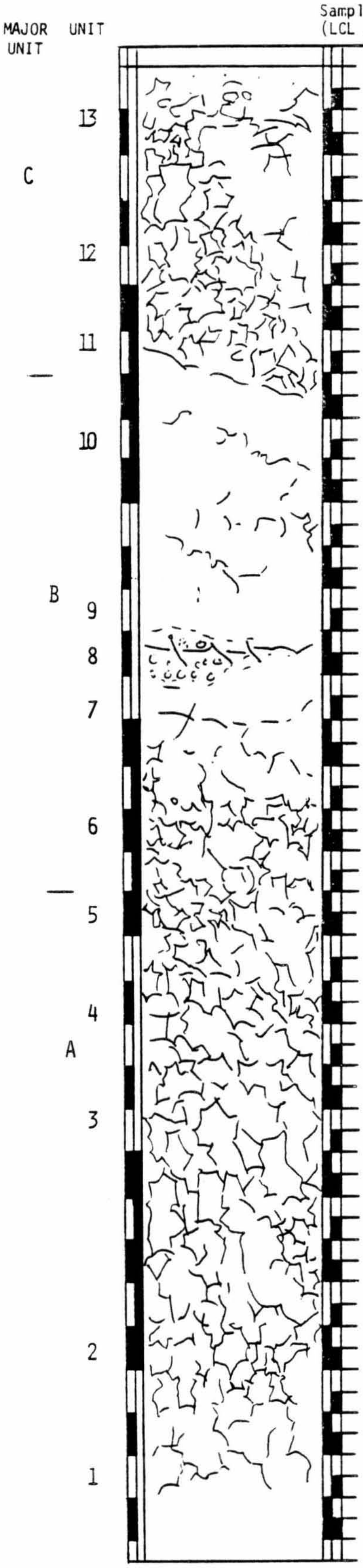

Sample Interval (LCL Inventory)	INTERVAL SAMPLES Sample No.	Vial No.	Sample Wt.	SPECIAL SAMPLES Sample No.	Vial No.	Sample Wt.	Sample Type
	removed previously						
0.0	2001	9-11201	3.735				
0.5	2002	9-11202	3.484				
1.0	2003	9-11203	4.712				
1.5	2004	9-11204	3.453				
2.0	2005	9-11205	4.302				
2.5	2006	9-11206	4.003				
3.0	2007	9-11207	4.921				
3.5	2008	9-11208	4.883				
4.0	2009	9-11209	4.575				
4.5	2010	9-11210	4.425				
5.0	2011	9-11211	4.488				
5.5	2012	9-11212	3.477				
6.0	2013	9-11213	4.044				
6.5	2014	9-11214	3.723				
7.0	2015	9-11215	4.678				
7.5	2016	9-11216	4.381				
8.0	2017	9-11217	4.216				
8.5	2018	9-11218	4.585				
9.0	2019	9-11219	4.441				
9.5	2020	9-11220	5.085				
10.0	2021	9-11221	4.851				
10.5	2022	9-11222	4.700				
11.0	2023	9-11223	3.421				
11.5	2024	9-11224	4.412				
12.0	2025	9-11225	4.735				
12.5	2026	9-11226	4.643				
13.0	2027	9-11227	4.039				
13.5	2028	9-11228	4.209				
14.0	2029	9-11229	4.356				
14.5	2030	9-11230	4.996				
15.0	2031	9-11231	4.097				
15.5	2032	9-11232	5.244				
16.0	2033	9-11233	4.002				
16.5	2034	9-11234	4.467				
17.0	2035	9-11235	4.483				
17.5	2036	9-11236	4.501				
18.0	2037	9-11237	4.400				
18.5	2038	9-11238	4.800				
19.0	2039	9-11239	3.936				
19.5	2040	9-11240	4.327				
20.0	2041	9-11241	4.198				
20.5	2042	9-11242	4.237				
21.0	2043	9-11243	5.095				
21.5	2044	9-11244	4.297	2045	9-11245	0.002	cpd.droplet
22.0	2046	9-11246	3.940				
22.5	2047	9-11247	4,518				
23.0	2048	9-11248	4.101				
23.5	2049	9-11249	4.412				
24.0	2050	9-11250	4.482				
24.5	2051	9-11251	3.811				
25.0	2052	9-11252	4.189				
25.5	2053	9-11253	4.583				
26.0	2054	9-11254	4.132				
26.5	2055	9-11255	4.519				
27.0	2056	9-11256	4.288				
27.5	2057	9-11257	4.507				
28.0	2058	9-11258	3.902				
28.5	2059	9-11259	4.652				
29.0	2060	9-11260	3.907				
29.5	2061	9-11261	4.382				
30.0	2062	9-11262	4.620				
30.5	2063	9-11263	3.606				
31.0	2064	9-11264	3.875				
31.5	2065	9-11265	4.098				
32.0	2066	9-11266	4.202				
32.5	2067	9-11267	3.218				
33.0	2068	9-11268	2.870				
33.4	2069	9-11269	3.667				
33.8	2070	9-11270	3.079				
34.3							

Fig. 19

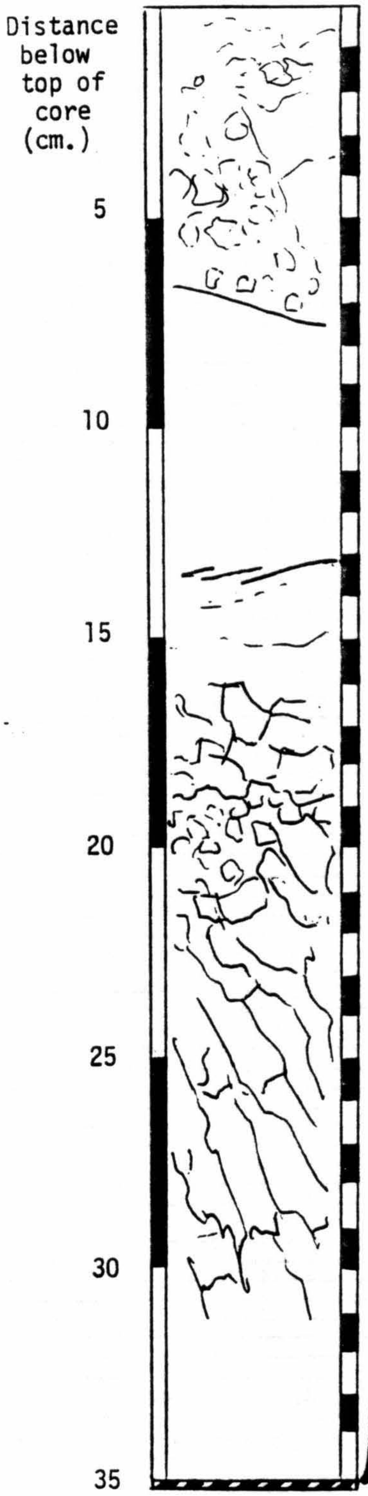

EARLY ALLOCATIONS FROM DRIVE TUBE 74001

Investigator and split received

Adams, JB	Burlingame, AL	Tatsumoto, M	Maurette, M	McKay, DS	Nava, D	Reed, GW	Wasserburg, GJ	Geiss, J	Uhlmann, DR	Anders, E	Sato, M
4	6	8	9	10	11	12	14	15	17	18	20
				2							

Material was removed from this portion of the core.

Fig. 20

ALLOCATIONS FROM CORE 74001

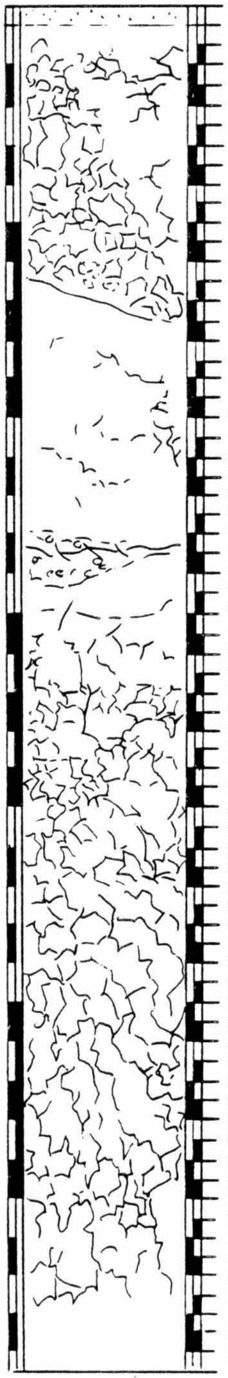

Investigator and splits received

Sample Interval (LCL Inventory)	PARENT SAMPLE	GÖSE, WA	ARNOLD, JR	GEISS, J	McKAY, DS	MEYER, C.	HOUSLEY, RM	REED, GW	THODE, HG
+.03	21	301			98	300			99
0.0	26	302							
0.5	27	303		100					
1.0	28	304		101					
1.5	29	305							
2.0	30	306							
2.5	31	307							
3.0	33	308							
3.5	34	309	103						
4.0	35	310					105	106	
4.5	36	311			107				
5.0	37	312							
5.5	38	313							
6.0	39	314							
6.5	40	315							
7.0	41	316							
7.5	42	317							
8.0	43	318							
8.5	44	319							
9.0	45	320				371			
9.5	46	321							
10.0	47	322		109					
10.5	48	323		110					
11.0	49	324					111	112	
11.5	50	325			113				
12.0	51	326							
12.5	52	327							
13.0	53	328							
13.5	54	329							
14.0	55	330							
14.5	56	331							
15.0	57	332							
15.5	58	333							
16.0	59	334							
16.5	60	335							
17.0	61	336	115						
17.5	62	337					117	118	
18.0	63	338			119	372			
18.5	64	339							
19.0	65	340							
19.5	66	341							
20.0	67	342							
20.5	68	343							
21.0	69	344							
21.5	70	345							
22.0	71	346							
22.5	72	347							
23.0	73	348							
23.5	74	349		121					
24.0	76	350		122					
24.5	77	351					123	124	
25.0	78	352			125				
25.5	79	353							
26.0	80	354							
26.5	81	355							
27.0	82	356				373			
27.5	83	357							
28.0	84	358							
28.5	86	359							
29.0	87	360							
29.5	88	361							
30.0	89	362							
30.5	90	363							
31.0	91	364							
31.5	92	365	127						
32.0	93	366					129	130	
32.5	94	367							
33.0	95	368							
33.5	96	369							
34.0 34.3	97	370							

Fig. 21

ALLOCATIONS FROM CORE 74001, DISS. 2

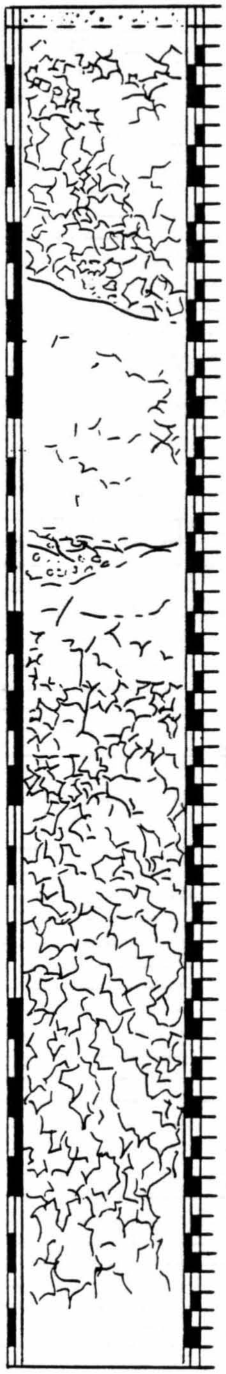

Investigator and splits received

Sample Interval (LCL Inventory)	PARENT SAMPLE	CLAYTON, RN	DEMARAIS, DJ	GIBSON, EK	MORGAN, JW	TILTON, GR	VON GUNTEN, HR	WASSON, JT
0.0								
0.5								
1.0								
1.5								
2.0	1004				1070			
2.5								
3.0								
3.5	1007		1071					
4.0	1008	1072						
4.5	1009					1074	1075	1073
5.0	1010			1076				
5.5								
6.0								
6.5								
7.0								
7.5								
8.0								
8.5								
9.0								
9.5	1019				1077			
10.0								
10.5								
11.0								
11.5	1023					1078	1079	
12.0	1024			1080				
12.5	1025		1081					
13.0	1026	1082						
13.5								
14.0								
14.5	1029							1083
15.0								
15.5								
16.0								
16.5								
17.0								
17.5								
18.0								
18.5								
19.0								
19.5								
20.0								
20.5								
21.0								
21.5								
22.0								
22.5								
23.0								
23.5								
24.0	1048		1084					
24.5	1049	1085						
25.0	1050				1086	1087	1088	
25.5	1051			1089				
26.0								
26.5								
27.0								
27.5								
28.0								
28.5								
29.0								
29.5								
30.0								
30.5								
31.0								
31.5								
32.0								
32.5	1065							1090
33.0								
33.5								
34.0								
34.3								

Fig. 22 LOCATION OF SAMPLES, FIRST (STANDARD) DISSECTION OF DRIVE TUBE 74002

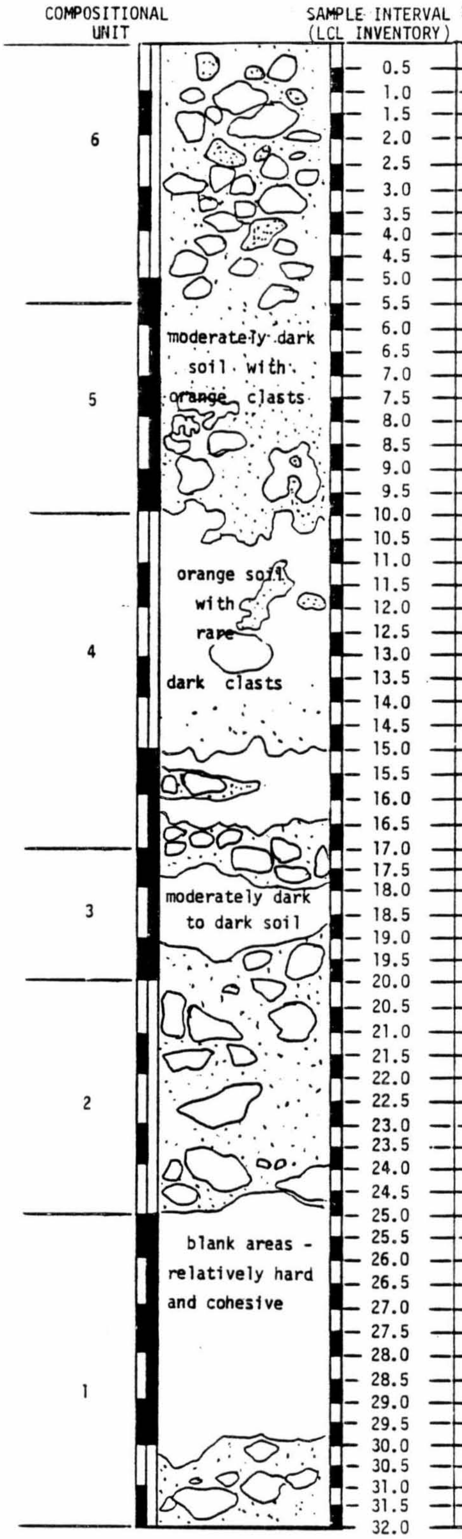

Sample No.	Vial No.	Sample wt.	Sample No.	Vial No.	Sample Wt.
See tables VIII, IX for top 5 mm					
89	9-10272	1.718	88	9-10271	0.605
87	9-10270	1.407			
86	9-10269	1.540	85	9-10268	0.926
84	9-10267	1.780			
82	9-10265	1.818	83	9-10266	0.614
80	9-10263	2.066	81	9-10264	0.816
78	9-10261	1.894	79	9-10262	0.622
77	9-10260	2.436			
76	9-10259	2.853			
74	9-10257	2.421	75	9-10258	0.384
73	9-10256	2.663			
72	9-10255	2.320			
71	9-10254	2.798			
70	9-10253	2.963			
69	9-10252	2.007			
68	9-10251	2.881			
67	9-10250	3.642			
66	9-10249	2.120			
65	9-10248	2.722			
63	9-10246	2.171	64	9-10247	0.739*
62	9-10245	2.548			
61	9-10244	3.082			
60	9-10243	2.183			
59	9-10242	2.075	58	9-10241	1.342*
57	9-10240	3.058	56	9-10239	0.702*
55	9-10238	2.137			
54	9-10237	2.696			
53	9-10236	2.344			
52	9-10235	2.729			
51	9-10234	2.344			
50	9-10233	3.024			
49	9-10232	2.839			
48	9-10231	2.730			
47	9-10230	2.923			
46	9-10229	3.059			
45	9-10228	3.104			
44	9-10227	2.638			
43	9-10226	2.647			
42	9-10225	2.946			
41	9-10224	2.882			
40	9-10223	2.903			
39	9-10222	2.911			
38	9-10221	2.639			
37	9-10220	3.218			
36	9-10219	2.943			
35	9-10218	2.698			
34	9-10217	2.818			
33	9-10216	2.958			
32	9-10215	3.326			
31	9-10214	3.391			
30	9-10213	2.861			
29	9-10212	2.750			
28	9-10211	3.653			
27	9-10210	2.809			
26	9-10209	2.858			
25	9-10208	2.840			
24	9-10207	2.872			
23	9-10206	2.594			
22	9-10205	3.243			
21	9-10204	2.911			
20	9-10203	3.092			
19	9-10202	3.368			
18	9-10201	3.442			

* These samples contain the most pure orange soil that could be extracted from the core

Fig. 23

LOCATION OF SAMPLES, SECOND (CHEMICALLY PURE) DISSECTION OF 74002

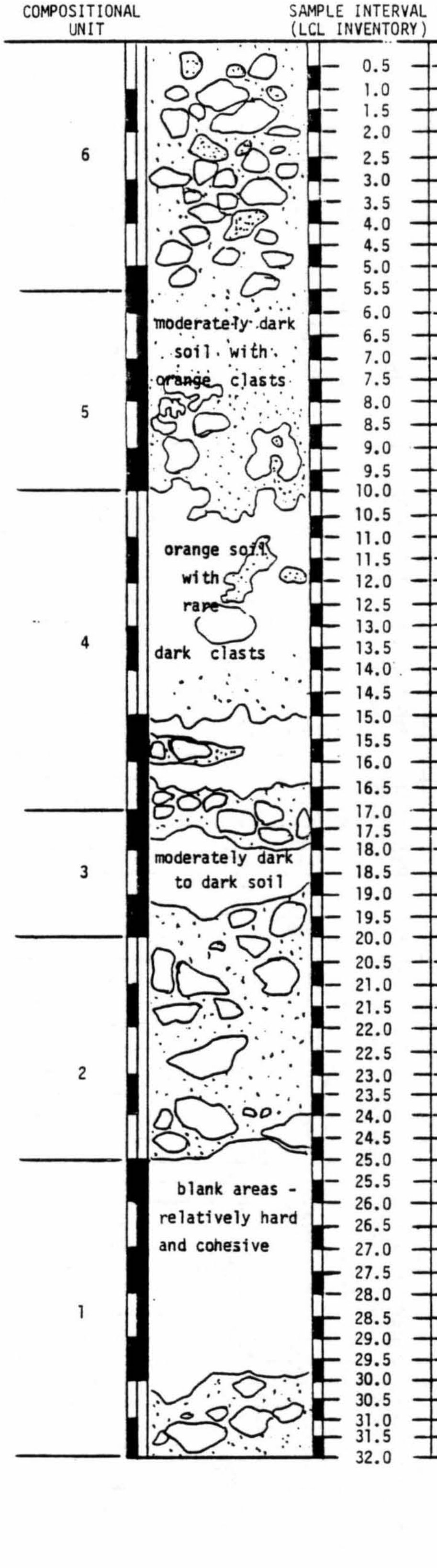

Sample No.	Vial No.	Sample Wt.
See tables VIII, IX		
1067	9-10367	1.832
1066	9-10366	2.798
1065	9-10365	2.751
1064	9-10364	2.748
1063	9-10363	3.245
1062	9-10362	4.105
1061	9-10361	3.782
1060	9-10360	2.991
1059	9-10359	2.651
1058	9-10358	2.867
1057	9-10357	3.154
1056	9-10356	3.520
1055	9-10355	3.626
1054	9-10354	3.985
1053	9-10353	3.511
1052	9-10352	3.575
1051	9-10351	3.854
1050	9-10350	3.668
1049	9-10349	3.426
1048	9-10348	3.736
1047	9-10347	3.859
1046	9-10346	3.174
1045	9-10345	4.473
1044	9-10344	3.329
1043	9-10343	3.773
1042	9-10342	4.156
1041	9-10341	3.924
1040	9-10340	3.519
1039	9-10339	3.039
1038	9-10338	4.009
1037	9-10337	3.323
1036	9-10336	2.912
1035	9-10335	2.950
1034	9-10334	3.666
1033	9-10333	3.942
1032	9-10332	3.810
1031	9-10331	3.290
1030	9-10330	3.389
1029	9-10329	3.530
1028	9-10328	3.402
1027	9-10327	4.229
1026	9-10326	3.269
1025	9-10325	3.855
1024	9-10324	3.707
1023	9-10323	3.950
1022	9-10322	3.625
1021	9-10321	3.236
1020	9-10320	3.411
1019	9-10319	3.581
1018	9-10318	4.402
1017	9-10317	3.475
1016	9-10316	3.821
1015	9-10315	3.195
1014	9-10314	3.613
1013	9-10313	4.846
1012	9-10312	3.960
1011	9-10311	4.413
1010	9-10310	3.593
1009	9-10309	3.520
1008	9-10308	4.748
1007	9-10307	3.203
1006	9-10306	3.886
1005	9-10305	2.756

Fig. 24 LOCATION OF SAMPLES, THIRD (STANDARD) DISSECTION OF DRIVE TUBE 74002

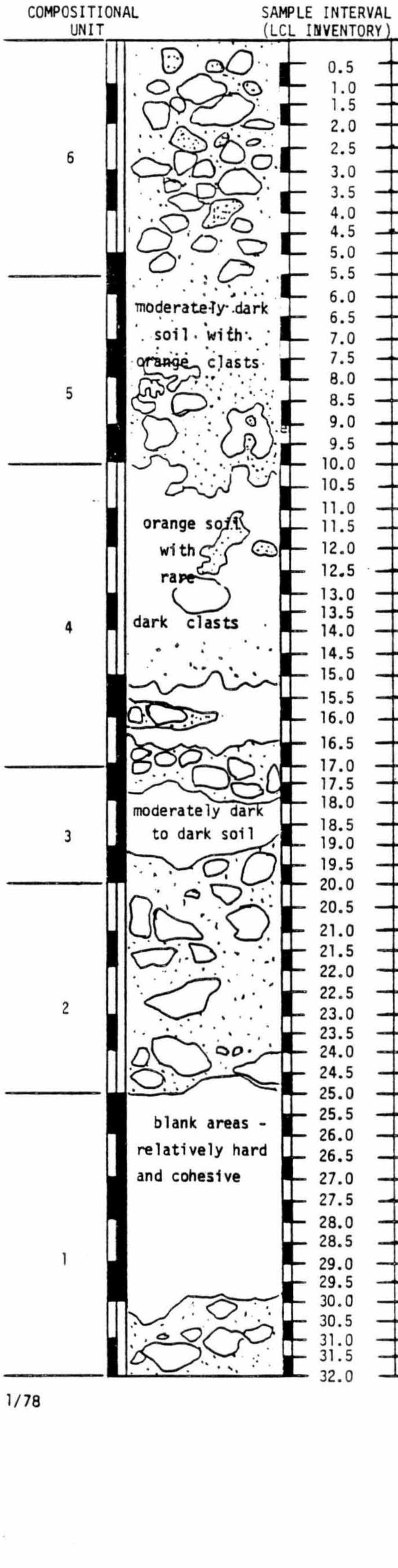

INTERVAL SAMPLES			COARSE FRACTION		
Sample No.	Vial No.	Sample Wt.	Sample No.	Vial No.	Sample Wt.
See tables VIII, IX for top 5 mm					
2070	9-11870	1.552	2071	9-11871	0.738
2068	9-11268	2.200	2069	9-11869	0.608
2066	9-11866	2.407	2067	9-11867	2.938
2064	9-11864	2.497	2065	9-11865	0.706
2062	9-11862	2.066	2063	9-11863	5.967
2061	9-11861	1.697			
2059	9-11859	2.690	2060	9-11860	3.622
2058	9-11858	1.912			
2056	9-11856	4.016	2057	9-11857	1.024
2055	9-11855	3.309			
2054	9-11854	4.269			
2053	9-11853	3.749			
2052	9-11852	3.754			
2051	9-11851	3.687			
2050	9-11850	3.993			
2049	9-11849	3.602			
2047	9-11847	3.148	2048	9-11848	1.108
2046	9-11846	3.956			
2045	9-11845	3.699			
2044	9-11844	4.149			
2043	9-11843	3.817			
2042	9-11842	3.669			
2041	9-11841	4.358			
2040	9-11840	3.559			
2039	9-11839	3.506			
2038	9-11838	4.400			
2037	9-11837	4.338			
2036	9-11836	4.004			
2035	9-11835	4.116			
2034	9-11834	4.232			
2033	9-11833	4.218			
2032	9-11832	3.801			
2031	9-11831	3.935			
2030	9-11830	4.033			
2029	9-11829	3.715			
2028	9-11828	4.467			
2027	9-11827	3.856			
2026	9-11826	3.875			
2025	9-11825	3.688			
2024	9-11824	3.930			
2023	9-11823	4.253			
2022	9-11822	3.877			
2021	9-11821	4.513			
2020	9-11820	3.966			
2019	9-11819	4.698			
2018	9-11818	3.528			
2017	9-11817	4.172			
2016	9-11816	4.340			
2015	9-11815	4.383			
2014	9-11814	3.989			
2013	9-11813	3.953			
2012	9-11812	4.351			
2011	9-11811	3.896			
2010	9-11810	4.792			
2009	9-11809	3.891			
2008	9-11808	4.538			
2007	9-11807	3.597			
2006	9-11806	3.364			
2005	9-11805	3.586			
2004	9-11804	3.991			
2003	9-11803	4.336			
2002	9-11802	3.643			
2001	9-11801	3.228			

Fig. 25 ALLOCATIONS FROM CORE

74002, DISSECTION 1

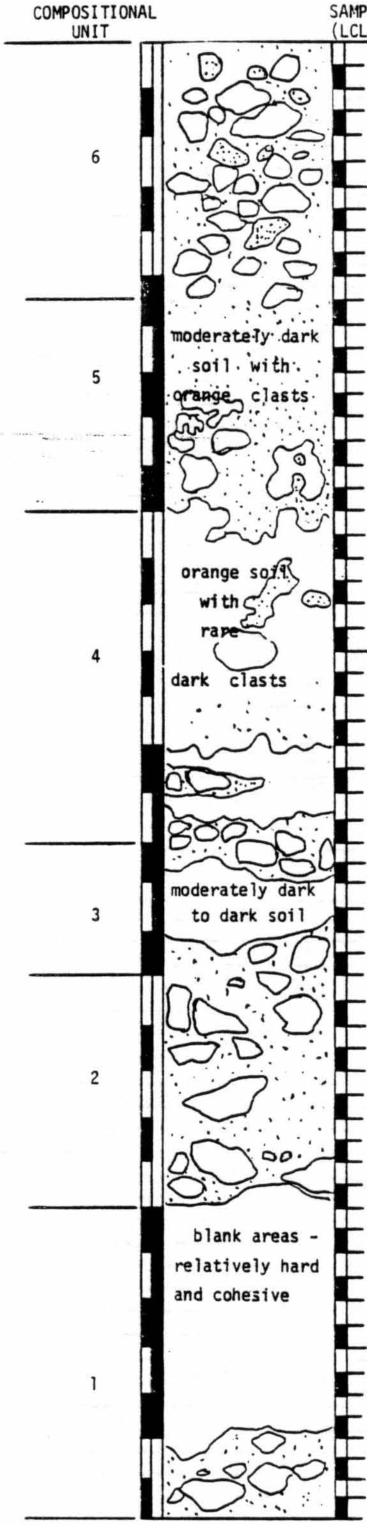

SAMPLE INTERVAL (LCL INVENTORY)	PARENT SAMPLES		Investigator and splits received
			Göse, W. A.
0.5–1.0	89		164
1.0–1.5	87		163
1.5–2.0	86		162
2.0–2.5	84		161
2.5–3.0	82		160
3.0–3.5	80		159
3.5–4.0	78		158
4.0–4.5			
4.5–5.0	76		157
5.0–5.5	74		156
5.5–6.0	73		155
6.0–6.5	72		154
6.5–7.0	71		153
7.0–7.5	70		152
7.5–8.0	69		151
8.0–8.5	68		150
8.5–9.0	67		149
9.0–9.5	66		148
9.5–10.0	65		147
10.0–10.5	63	64	145,6
10.5–11.0	62		144
11.0–11.5	61		143
11.5–12.0	60		142
12.0–12.5	59	58	141,0
12.5–13.0	57	56	139,8
13.0–13.5	55		137
13.5–14.0	54		136
14.0–14.5	53		135
14.5–15.0	52		134
15.0–15.5	51		133
15.5–16.0	50		132
16.0–16.5	49		131
16.5–17.0	48		130
17.0–17.5	47		129
17.5–18.0	46		128
18.0–18.5	45		127
18.5–19.0	44		126
19.0–19.5	43		125
19.5–20.0	42		124
20.0–20.5	41		123
20.5–21.0	40		122
21.0–21.5	39		121
21.5–22.0	38		120
22.0–22.5	37		119
22.5–23.0	36		118
23.0–23.5	35		117
23.5–24.0	34		116
24.0–24.5	33		115
24.5–25.0	32		114
25.0–25.5	31		113
25.5–26.0	30		112
26.0–26.5	29		111
26.5–27.0	28		110
27.0–27.5	27		109
27.5–28.0	26		108
28.0–28.5	25		107
28.5–29.0	24		106
29.0–29.5	23		105
29.5–30.0	22		104
30.0–30.5	21		103
30.5–31.0	20		102
31.0–31.5	19		101
31.5–32.0	18		100

Fig. 26 ALLOCATIONS FROM CORE 74002, DISSECTION 2

COMPOSITIONAL UNIT

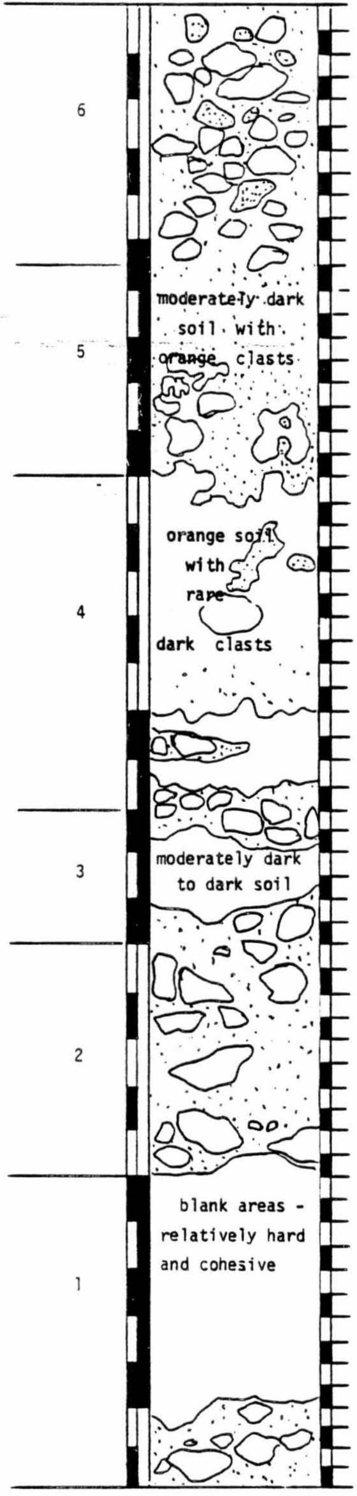

Investigator and Splits Received

SAMPLE INTERVAL (LCL INVENTORY)	PARENT SAMPLE	Gibson, EK.	Housley, RM	Reed, GW	Wasson, JT	
0.5–1.0	1067					
1.0–1.5	1066					
1.5–2.0	1065					
2.0–2.5	1064			1068		
2.5–3.0	1063		1069			
3.0–3.5	1062					
3.5–4.0	1061					
4.0–4.5	1060			1070		
4.5–5.0	1059					
5.0–5.5	1058	1071			1072	
5.5–6.0	1057	1073			1074	
6.0–6.5	1056	1075		1076	1077	
6.5–7.0	1055	1078			1079	
7.0–7.5	1054		1080			
7.5–8.0	1053					
8.0–8.5	1052			1081		
8.5–9.0	1051					
9.0–9.5	1050					
9.5–10.0	1049					
10.0–10.5	1048					
10.5–11.0	1047					
11.0–11.5	1046					
11.5–12.0	1045			1082		
12.0–12.5	1044					
12.5–13.0	1043		1083			
13.0–13.5	1042					
13.5–14.0	1041	1084			1085	
14.0–14.5	1040	1086			1087	
14.5–15.0	1039	1088			1089	
15.0–15.5	1038	1090			1091	
15.5–16.0	1037					
16.0–16.5	1036					
16.5–17.0	1035					
17.0–17.5	1034					
17.5–18.0	1033		1092			
18.0–18.5	1032	1093			1094	
18.5–19.0	1031	1095			1096	
19.0–19.5	1030	1097			1098	
19.5–20.0	1029	1099			1100	
20.0–20.5	1028					
20.5–21.0	1027					
21.0–21.5	1026					
21.5–22.0	1025					
22.0–22.5	1024					
22.5–23.0	1023		1101			
23.0–23.5	1022			1102		
23.5–24.0	1021					
24.0–24.5	1020					
24.5–25.0	1019					
25.0–25.5	1018					
25.5–26.0	1017			1103		
26.0–26.5	1016					
26.5–27.0	1015	1104			1105	
27.0–27.5	1014	1106			1107	
27.5–28.0	1013	1108		1109	1110	
28.0–28.5	1012	1111			1112	
28.5–29.0	1011		1113			
29.0–29.5	1010					
29.5–30.0	1009			1114		
30.0–30.5	1008					
30.5–31.0	1007					
31.0–31.5	1006			1115		
31.5–32.0	1005					

Fig. 27

ALLOCATIONS FROM CORE 74002, DISSECTION 3

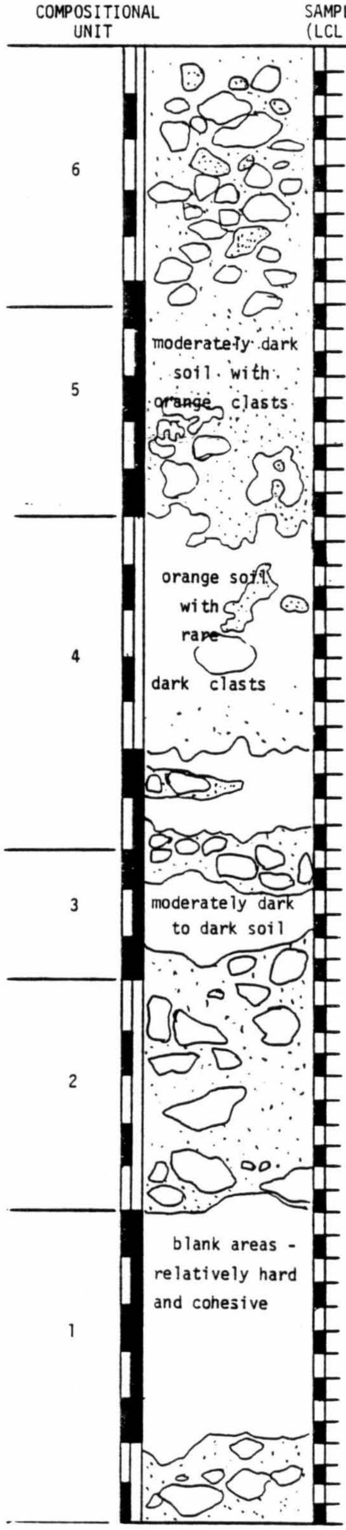

SAMPLE INTERVAL (LCL INVENTORY)	PARENT SAMPLE	Investigator and Splits Received					
		Arnold, JR	Clayton, RN	Geiss, J	Walker, RM	Sato, M	
0.5							
1.0	2070	2073					
1.5	2068	2074					
2.0	2066	2075					
2.5	2064	2076					
3.0	2062	2077			2078		
3.5	2061	2079					
4.0	2059						
4.5	2058						
5.0	2056	2080					
5.5	2055		2081	2082			
6.0	2054		2083	2084			
6.5	2053		2085	2086			
7.0	2052		2087	2088			
7.5	2051	2090			2091		
8.0	2050						
8.5	2049						
9.0	2047						
9.5	2046						
10.0	2045						
10.5	2044	2092					
11.0	2043						
11.5	2042						
12.0	2041						
12.5	2040						
13.0	2039				2093		
13.5	2038					2094	
14.0	2037		2095	2096			
14.5	2036		2097	2098			
15.0	2035		2099	2100			
15.5	2034		2101	2102			
16.0	2033						
16.5	2032						
17.0	2031						
17.5	2030						
18.0	2029				2103		
18.5	2028		2104	2105			
19.0	2027		2106	2107			
19.5	2026		2108	2109			
20.0	2025		2110	2111			
20.5	2024						
21.0	2023						
21.5	2022						
22.0	2021						
22.5	2020						
23.0	2019				2112		
23.5	2018						
24.0	2017						
24.5	2016						
25.0	2015						
25.5	2014						
26.0	2013						
26.5	2012						
27.0	2011		2113	2114			
27.5	2010		2115	2116			
28.0	2009		2117	2118			
28.5	2008		2119	2120			
29.0	2007				2121		
29.5	2006						
30.0	2005						
30.5	2004						
31.0	2003						
31.5	2002						
32.0	2001						